Remote Sensing of Environment 339 (2026) 115389

Contents lists available at ScienceDirect

Remote Sensing of Environment

journal homepage: www.elsevier.com/locate/rse

European Ground Motion Service: A decade of Sentinel-1 observations☆

M. Crosetto [a,*], M. Cuevas-González [a], M. Mróz [b], D.A. Moldestad [c], F. Raspini [d], N. Casagli [d], L. Bateson [e], A. Novellino [e], M. Motagh [f,g], L. Guerrieri [h], V. Comerci [h]

[a] Centre Tecnològic de Telecomunicacions de Catalunya (CTTC/CERCA), Geomatics Division, Av. Gauss, 7, E-08860 Castelldefels, Barcelona, Spain
[b] Institute of Geodesy and Civil Engineering, University of Warmia and Mazury in Olsztyn, ul. Oczapowskiego 1, 10-719 Olsztyn, Poland
[c] Norsk Romsenter, Drammensveien 165, 0277 Oslo, Norway
[d] University of Firenze, Department of Earth Sciences, Via La Pira 4, 50121 Firenze, Italy
[e] British Geological Survey, Nicker Hill, Keyworth, Nottingham NG12 5GG, United Kingdom
[f] Section of Remote Sensing and Geoinformatics, GFZ Helmholtz Centre for Geosciences, Helmholtz-Zentrum, Potsdam, Germany
[g] Institute of Photogrammetry and Geoinformation, Leibniz University Hannover, Hannover, Germany
[h] Istituto Superiore per la Protezione e la Ricerca Ambientale - ISPRA, Via Vitaliano Brancati, 48, 00144 Roma, Italy

ARTICLE INFO

Edited by Marie Weiss

Keywords:
European Ground Motion Service
EGMS
Copernicus
Persistent Scatterer Interferometry
SAR
Sentinel-1
Displacement
Deformation
User uptake
Service evolution

ABSTRACT

This work is focused on the European Ground Motion Service (EGMS), a Copernicus service based on the Persistent Scatterer Interferometry technique and satellite Synthetic Aperture Radar imagery from Sentinel-1. The EGMS provides displacement measurements related to both natural and anthropogenic ground motion phenomena, which are standardized and harmonized across national borders over Europe. For its characteristics, EGMS represents one of the most important initiatives of this type worldwide. At the beginning of this paper, the main characteristics of EGMS are described, considering the main technical aspects involved in the service. Then, the user uptake of the service is considered by addressing three different aspects: download of the EGMS data, publication in the scientific literature, and usage beyond the academic domain. These aspects indicate a growing recognition of EGMS as a valuable tool for understanding ground deformation processes. The published studies demonstrate the wide-ranging utility of EGMS data across various applications, extending beyond academic research and benefitting also public bodies and private companies. A key section of the paper describes five representative EGMS applications. Two studies concern local areas, while the other ones involve wide-area EGMS data and analyses on national scale, with the potential to be extended to the entire continent. In the last part of the paper, the evolution of EGMS is addressed. A stepwise extension of EGMS towards global coverage is foreseen, creating the so-called Copernicus Global Ground Motion Service (CGGMS). A roadmap for the EGMS extension to CGGMS is outlined, starting from Europe up to reaching a global scale. Other aspects include the use of L-band data from ROSE-L and NISAR, and C-band data from Sentinel-1 Next Generation data.

1. Introduction

This paper concerns the European Ground Motion Service (EGMS), a service based on Persistent Scatterer Interferometry (PSI, see Crosetto et al., 2016) and Synthetic Aperture Radar (SAR) imagery, which is part of the European Union Copernicus Programme. EGMS has a European continental coverage, and this makes it one of the most important initiatives of this type worldwide. The realization of this service has been preceded by a long development, which occurred in the last three decades.

This development started in the 90s, with the availability of SAR data from the ESA satellites ERS-1 (1991–2011) and ERS-2 (1995–2011). In the decade 1991–2001, several Differential Interferometric SAR (DInSAR) techniques were developed, and several DInSAR applications were demonstrated, e.g. see Hanssen (2001). In 2000, a major step forward was made with the introduction of the first PSI technique (Ferretti et al., 2000, 2001). The following decade, approximately from 2001 to 2012 saw the development of several new algorithms (Berardino et al., 2002;

☆ This article is part of a Special issue entitled: 'Ten years of Sentinel-1 in space (Invitation Only)' published in Remote Sensing of Environment.

* Corresponding author.
E-mail addresses: mcrosetto@cttc.cat (M. Crosetto), mcuevas@cttc.cat (M. Cuevas-González), marek.mroz@uwm.edu.pl (M. Mróz), dag.anders.moldestad@spaceagency.no (D.A. Moldestad), federico.raspini@unifi.it (F. Raspini), nicola.casagli@unifi.it (N. Casagli), lbateson@bgs.ac.uk (L. Bateson), alessn@bgs.ac.uk (A. Novellino), mahdi.motagh@gfz.de (M. Motagh), luca.guerrieri@isprambiente.it (L. Guerrieri), valerio.comerci@isprambiente.it (V. Comerci).

https://doi.org/10.1016/j.rse.2026.115389
Received 21 March 2025; Received in revised form 6 November 2025; Accepted 24 March 2026
Available online 2 April 2026

Mora et al., 2003; Werner et al., 2003; Hooper et al., 2004; Costantini et al., 2008; Ferretti et al., 2011), which were mainly based on ERS-1/2 and Envisat (2002−2012) SAR imagery. In the same period, the fields of application of PSI were widely extended and consolidated (see e.g. Lauknes et al., 2010; Crosetto et al., 2016), national scale InSAR services were planned (Strøm et al., 2014; Kalia et al., 2017) and started to develop (Dehls et al., 2019), culminating with the planning (EGMS White Paper, 2017), specification (Larsen et al., 2020) and production of the EGMS (Kotzerke et al., 2022; Capes and Passera, 2023; Ferretti et al., 2025), see for an overview Crosetto et al. (2020) and Crosetto and Solari (2023).

The last decade was marked by the advent of the Sentinel-1 A (2014-ongoing) and 1B (2016–2021) sensors. The Sentinel-1 (S-1) missions are characterized by wide-area and repetitive observations, a high-capacity ground segment, and a free and open data policy. The availability of S-1 SAR data represented a game changer for many PSI applications, with an extraordinary increase of acquisition capability, spatially and temporally. This capability allows global data acquisition coverage and is fully deployed over Europe. With the availability of both S-1 A and S—1B, an acquisition every at least 6 days for both ascending and descending geometries was guaranteed in any place of the continent. After the failure of S—1B (23 December 2021), the rate was at least one acquisition every 12 days. The 6-day scenario has been restored after the end of the commissioning phase of S—1C (May 2025), which was launched on 5 December 2024.

Data availability and the readiness of mature PSI processing and analysis tools are key components for the development of a service like EGMS. In the last years this was accompanied by the accessibility of powerful computational resources, and the development of advanced visualization platforms (Crosetto et al., 2025). All these enablers were finally jointly exploited when fundings were secured by the European Union to make EGMS happens in the framework of the Copernicus Programme.

The implementation and maintenance of EGMS require a major economic and technical effort. This paper describes the service and investigates its impact. Section 2 starts with a description of EGMS. This is followed by a discussion of the main technical aspects involved in the service. Section 4 concerns the EGMS user uptake, considering data download, the scientific literature, and the usage beyond the academic domain. An important section is devoted to the discussion of five applications with the objective of illustrating the EGMS potential. The paper closes with a discussion of the foreseen evolution of EGMS and the paper conclusions.

2. European Ground Motion Service

The EGMS provides displacement measurements related to both natural and anthropogenic ground motion phenomena, which are standardized and harmonized across national borders over Europe. The service is based on the processing of full resolution S-1 SAR data using PSI techniques, which exploit both point-like and distributed scatterers (Crosetto and Solari, 2023). In this paper, we use the term PSI to indicate both point-like and distributed scatterer techniques, and Measurement Points (MPs) to refer collectively to both point-like and distributed scatterers. The EGMS represents one of the most important services devoted to land deformation measurement worldwide. Its products are made available on a full, open, and free-access basis.

The PSI measurements produced by EGMS include the results of a baseline processing, which covered the 2015–2020 period and was published in 2021. This is followed by annual updates, which to date covered 2015–2021, published in 2022; 2018–2022, published in 2023; and 2019–2023, published in 2024. The observation periods are adjusted, rather than simply expanded, to prevent the loss of many MPs. Concerning the spatial extent of EGMS, it covers most of Europe by including all the Copernicus participating states: Austria, Belgium, Bulgaria, Croatia, Cyprus, Czech Republic, Denmark, Estonia, Finland, France, Germany, Greece, Hungary, Ireland, Italy, Latvia, Lithuania, Luxembourg, Malta, the Netherlands, Poland, Portugal, Romania, Slovakia, Slovenia, Spain, Sweden, United Kingdom, Iceland, and Norway.

The EGMS products are accessible through the EGMS Explorer at https://egms.land.copernicus.eu, which offers two main functionalities: an interactive WebGIS to visualize EGMS products and perform basic data analysis operations (see e.g. Larsen et al., 2023), and an interface0 to search and download EGMS products, which can only be accessed by registered users. Through the EGMS Explorer the user can access a comprehensive technical documentation.

The EGMS is part of the Copernicus Land Service and is managed by the European Environment Agency. Its activity is overseen by the Advisory Board, which is composed of the authors of this paper. The EGMS production is made by e-GEOS, TRE Altamira, the Geological Survey of Norway (NGU), NORCE, PPO.labs, DLR, and GAF and the Satellite Geodetic Observatory. Finally, an independent team is responsible for the EGMS validation activities. The EGMS consortium operates four different PSI chains. Harmonization among such chains was achieved through work on a representative test area, with the goal of delivering results that are comparable in terms of quality and MP densities. A test area exceeding 46,000 km^2 was selected to implement new solutions and fine-tune several processing parameters to satisfy the project requirements. MP spatial density was the most critical parameter to be adjusted. Harmonization was achieved by tuning the threshold for the maximum root mean square error allowed in the deformation time series, and by performing some adjustments to the algorithms used for selecting MP candidates. Within the test area, the resulting MP densities showed average differences of approximately 10% (Ferretti et al., 2025, page 55).

3. EGMS from a technical viewpoint

The EGMS includes three main PSI products, see for more details Larsen et al. (2020). The first one, named Basic product, contains line-of-sight (LOS) deformation velocity and time series for each MP. The Basic product is delivered for individual data blocks, which correspond to the burst geometry of the original S-1 SAR images. Each location is covered by two Basic products, corresponding to the ascending and descending geometries. Measurements in the Basic product are referenced to a local virtual reference point: the displacement data are referred to the mean or mode value of the dataset (Ferretti et al., 2025). In the second product, named Calibrated product, the Basic data blocks are mosaicked and referenced to a deformation velocity model derived from GNSS data (Dehls et al., 2022), offering absolute deformation values rather than relative measurements. Finally, the Ortho product includes two motion components for each MP: East-West horizontal and up/down vertical. For each MP, the Ortho product provides deformation velocity and time series that are referenced to the same GNSS deformation model used in the Calibrated product. The Ortho product has a lower resolution with respect to the other two products: it is resampled to a 100 m grid.

It is worth underlining the fundamental role that the GNSS deformation velocity model plays to derive the Calibrated and Ortho products. This model is estimated over a 50-km grid starting from thousands of GNSS permanent stations distributed over Europe (Marinkovic et al., 2024). The integration of PSI and GNSS measurements allows the Calibrated and Ortho products to include detailed and local-scale relative measurements (up to tens of kilometres) coming from PSI, along with absolute measurements over much larger extents (up to several thousands of kilometres) coming from GNSS stations. Starting from the fourth update (2020–2024), the GNSS component for each MP will be included in the Calibrated and Ortho products, therefore made available to users upon download. In addition, the EGMS Explorer will allow users to visualize the Calibrated and Ortho products either with or without the GNSS-derived long-wavelength component.

The EGMS uses most of the S-1 imagery acquired over Europe in the

last decade. The baseline processing and the first update took advantage of the 6-day repeat cycle ensured by S-1 A and S—1B. This represents a rather dense temporal sampling for many deformation phenomena, which involved the processing of over 33,000 bursts. The total amount of uncompressed S-1 data used for the baseline analysis was about 1.5 PB. Starting from 23 December 2021 one satellite only was available, acquiring with a 12-day cycle. Spatially, EGMS provides a massive sampling. The Calibrated product included over 10 billion points in the baseline processing and over 15 billion points in the third update (2019–2023).

The EGMS is designed as a general-purpose service. Unlike localized processing tailored to specific end-users and a set of predefined user requirements, EGMS performs processing at a continental scale. However, as discussed in Section 4, the service supports a variety of applications. Additionally, if a specific application requires ad hoc processing, using the same S-1 data or alternative SAR datasets (e.g. X-band or L-band), this can be carried out to complement the EGMS products. A limitation of the EGMS is its delay in product delivery. In fact, due to massive processing workload, EGMS updates are only published annually, usually after summer. This implies that there is always a delay between 8 and 20 months between the date of the last processed SAR image and the present. Therefore, EGMS products cannot be used to monitor recent deformation events. This gap of 8–20 months can be filled by processing the most recent S-1 data or using other types of SAR imagery to complement EGMS products.

Another limitation concerns major earthquakes and active volcanic areas. These events cause large, anomalous deformation fields that may not be appropriately captured using the standard EGMS processing workflow. To address this issue, all major events are identified using dedicated catalogues, and a custom processing strategy is applied. First, the main deformation field is estimated at coarse resolution using traditional InSAR techniques. Second, this field is removed from the interferograms concerned (i.e. these interferograms are flattened). Third, the standard EGMS processing is then performed on the flattened interferograms, after which the main deformation field is reintroduced to reconstruct the complete deformation time series (Kotzerke et al., 2024).

3.1. EGMS validation activities

Validation is essential for ensuring the reliability, accuracy, and usability of the EGMS products. Each EGMS update is appropriately validated, with results publicly available (Sala et al., 2023). Quality assurance and control activities by the production consortium ensure compliance with EGMS specifications (Kotzerke et al., 2024). Validation activities performed across various European sites measure agreement between EGMS and reference data from ground-based and Earth Observation sources. Two main criteria guide the process: (1) consistency and accuracy, and (2) applicability and usability. Consistency and accuracy are assessed by comparing EGMS velocities and time series with GNSS and in-situ data. Applicability and usability evaluate the qualitative consistency of EGMS measurements with other Ground Motion Services (GMS) and geological information exploiting, for example, the concept of Active Deformation Areas (ADAs).

The last validation report (Koudogbo et al., 2025) confirms that EGMS products generally meet technical standards and effectively support diverse ground motion monitoring applications. EGMS captures mining-induced motion, groundwater-related subsidence, and urban deformations, such as in Lorca, Oslo, and Thyborøn, showing strong correlations with reference datasets. EGMS Basic and Calibrated products accurately delineate landslide areas, with around 50% of ADAs intersecting existing inventories in France and Spain. Despite low point density in vegetated areas, EGMS reliably detects and tracks slow-moving landslides. In the Alpes Maritimes, more than half of the potential landslides identified by EGMS are not recorded in the up-to-date national landslide inventory, particularly slow-moving landslides, offering valuable insights for updating national inventories. In Italy and Norway, EGMS results align well with GMS, corner reflectors, and GNSS data, with velocity differences typically below 1 mm/year. In volcanic areas such as Etna and La Palma, EGMS results show mixed performance under complex conditions. For Etna, although differences exist between EGMS and reference products, the overall correspondence between datasets is considered good for such a highly dynamic volcanic environment, indicating EGMS's potential to map displacements under challenging conditions. In La Palma, the descending orbit of the Basic products performs relatively better, showing a reasonable ability to reproduce GNSS displacement time series. This represents progress towards improving EGMS performance in active volcanic regions. Given the non-linear nature of deformation associated with eruptions, the Basic products remain the most suitable option for such analyses. Although some challenges remain, EGMS demonstrates consistency, accuracy, and robustness in mapping both long-term and seasonal ground movements, confirming its suitability for operational use in monitoring landslides, mining, groundwater exploitation, urban settlements, and volcanic deformation. It is, however, essential to carefully select the most appropriate EGMS product for each specific application. For detailed information on specific validation activities, refer to the available validation reports (Sala et al., 2023, 2024; Koudogbo et al., 2025).

4. EGMS user uptake

We consider in this section different aspects that can be used to assess the EGMS user uptake. A first insight is given by the statistics on EGMS data download. As it is shown in Fig. 1, between 2023 and 2024, the average zipped data download was 7.22 TB/quarter. For the update 2015–2021, the zipped Basic product for all Europe, both ascending and descending, was 3.39 TB. Given that there are thousands of data requests per quarter, the downloads mainly concern local studies, i.e. single or a few bursts. The approximate coverage of one burst is 20 by 80 km. A similar behaviour is shown by the Ortho product. The average zipped data download is 392 GB/quarter, while the zipped Ortho product for all Europe is about 80 GB. Again, the occurrence of thousand downloads per quarter imply that the users typically download single 100 by 100 km tiles of reduced groups of tiles.

The importance of EGMS is witnessed by the number of tools and procedures that have been proposed for data analysis and exploitation. This includes tools for extraction and conversion of data (Festa and Del Soldato, 2023; Hrysiewicz et al., 2024); tools for data clustering (Barra et al., 2017); automatic classification of such clusters (Navarro et al., 2020; Palamà et al., 2024; Rivera-Rivera et al., 2024); assessment of the potential impact of the detected clusters (Zêzere et al., 2024); tools to analyse time series (Evers et al., 2023; Kuzu et al., 2023); and tools to analyse spatial differential deformations (Shahbazi et al., 2022, 2024).

The impact of EGMS is shown by the number of papers published in the scientific literature. A total of 89 papers have been identified, which are reported in Table 1. The number of publications is increasing exponentially: 1 publication in 2021, 2 in 2022, 24 in 2023 and 62 in 2024. This clearly shows that the number of academic users is getting larger and larger.

As one may notice from Table 1, the domains of applications of EGMS are various, confirming the multi-purpose nature of EGMS. The most studied application fields are landslides (24%), followed by infrastructures (21%) and subsidence (19%).

It is interesting to note that most of the published studies are based on the Ortho product. Out of 64 papers with identified product type, 47 (i.e. 73%) use the Ortho product, with 36 of them using exclusively it. The Ortho product is surely the easiest EGMS product, especially the one that concerns the up/down vertical motion. This probably explain its wide use. It is however useful to underline that the other two EGMS products offer a remarkably higher spatial resolution, which can help any study devoted to small deformation phenomena, e.g. small

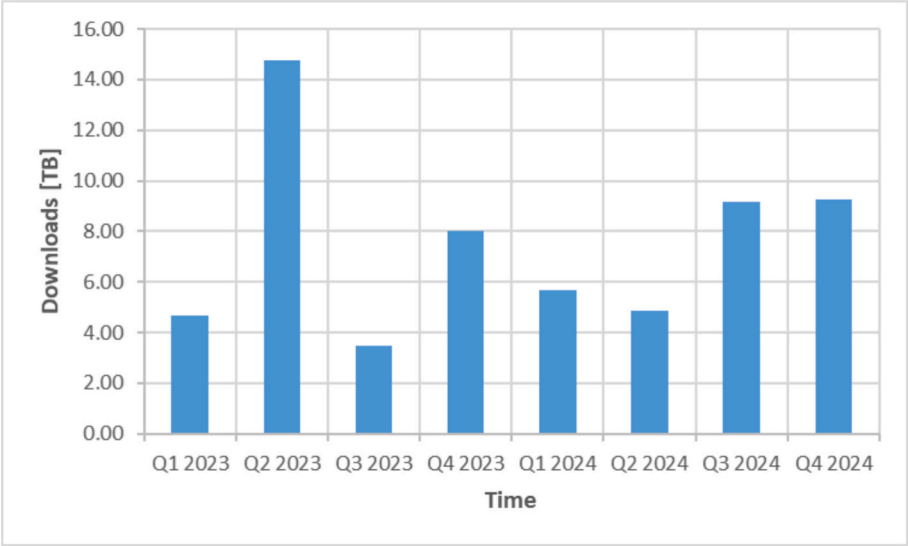

Fig. 1. EGMS data downloads in TB organized by quarters.

landslides, buildings, infrastructures, etc.

Besides the use in the academy, the EGMS is getting used by public bodies and private companies. Without the aim of being exhaustive, in the following we list some examples.

- Adamski et al. (2024) describe the integration of the Ortho product into products of the Polish Geological Survey (PGS). This includes the interpretation of major Polish deformation phenomena, and the publication of the EGMS Ortho data in the PGS geoportal.
- Even et al. (2024b) mention some initiatives of surveying authorities to complement their portfolios by including products from the German Ground Motion Service and EGMS. They foresee a key role for surveying authorities as an interface between EGMS and different technical administrations.
- Different examples of exploitation of EGMS data can be found at Italian regional level. Examples include the support in landslide monitoring for the technical services in Apulia (Sonnessa, 2024) and Piedmont (Regione Piemonte, 2024).
- CNR IRPI (2024) describes the use of EGMS data to update and reclassify the landslide phenomena for the Plan for Hydrogeological Management of the Po River Basin District.
- ANAS, the company in charge of road infrastructure in Italy, makes use of EGMS data to monitor the slopes and infrastructures that interest its road network (Strade and Autostrade, 2024).
- Detektia, a Spanish company specialized in PSI services, has developed an inventory of EGMS applications to civil engineering (Detektia, 2024). They propose a multi-source procedure to perform an integrated deformation analysis.
- Finally, GeoKinesia, another Spanish PSI company, offers a webmap service that includes two layers derived from EGMS (https://geokinesia.com/european-ada/). The first one includes the cluster of active deformation areas of Europe, while the second one includes the map of differential deformations over the Catalonia region (Spain).

5. Discussion of EGMS/based case studies

In this section we describe some relevant case studies that are useful to illustrate the characteristics and potential of the EGMS products. The first two studies concern local areas. The first one is focused on surface displacements caused by mining activities. It includes a comparison of the EGMS Calibrated products with PSI results from very high-resolution SAR data. The second one includes the analysis of volcanic features in the Mount Etna area.

The last three studies involve wide-area EGMS data. They are useful to perform homogeneous analysis at national scale, with the potential to be extended to the entire continent. The first study concerns the classification of moving areas in Italy. The second one involves a nation-wide analysis study on the correlation of coastal ground deformation with land cover and geology. The third study is focused on differential ground deformation in Spain.

5.1. *Mining-induced deformation*

Land subsidence caused by extensive coal mining is a critical issue affecting many urban areas worldwide. In such areas, geological faults are particularly vulnerable to reactivation (Donnelly, 2006). This can lead to the formation of scarps and fissures, which can cause damage to civil-engineered infrastructure and the surrounding land (Donnelly, 2000). Displacements along reactivated faults may significantly undermine the structural integrity of buildings and underground utilities, creating risks to the safety of residents and their properties.

In Germany, such a process is common in the Rhineland Coalfield, which is the largest lignite-producing area in Europe (Tang et al., 2020), located in the densely populated state of North Rhine-Westphalia, between the cities of Aachen and Cologne. We consider three large open-pit mines—Hambach, Garzweiler, and Inden. The EGMS data from Fig. 2a delineate well the extension of the subsidence area in the region. Such data can be utilized to quantify differential settlement, and evaluate hazards and risk related to subsidence and faulting surrounding the open-pit mines. Fig. 2b illustrates angular distortion estimated from Fig. 2a (Vassileva et al., 2021). In this figure, the spatial distribution of high angular distortion areas correlates well with the distribution and trace of mapped faults, indicating the role of geological factors and pre-existing stress fields in localizing deformation and creating steep gradients in differential settlements (Motagh et al., 2017; Cigna and Tapete, 2021). Interestingly, field surveys conducted during 2021–2024 documented many examples of damage due to fault reactivation and differential settlement in the housing and road surfaces of the area (Fig. 2c-e).

To evaluate the quality of EGMS products, a comparison was made between the Calibrated product and PSI results from TerraSAR-X (TSX) for the Hambach open-pit mine (Fig. 3a-b). 124 TSX images in a descending orbit between 2017/09/14 and 2022/01/04 were analyzed using the SARvey software (Piter et al., 2024). The average difference between the two datasets was removed to account for different reference points. Fig. 3c-d illustrate the correlation and differences between the

Table 1
EGMS papers published in the literature. In the references column, **/B** indicates the use of the EGMS Basic, **/C** the Calibrated product, and **/O** the Ortho. This is not specified when the information is unavailable.

Topic	References
Land subsidence in coastal areas & relative sea level rise	Antoniadis et al. (2023)/O, Thiéblemont et al. (2024)/O, Melet et al. (2021)/O, Evelpidou et al. (2023)/O, Cappucci et al. (2024)/O
Subsidence phenomena	Hasan et al. (2023)/O, Mateos et al. (2024), Khan et al. (2024), Beccaro et al. (2023)/O, Ghaderpour et al. (2024)/C,O, Ghaderpour et al. (2024b)/O, Farías et al. (2024)/O, Leone et al. (2024)/O, Cigna et al. (2024)/O, Zuccarini et al. (2024)/C, Righini et al. (2024)/B,C,O, Bru et al. (2024)
Local landslide studies	Yishu (2022)/O, Nikolakopoulos et al. (2023)/O, Godone et al. (2023)/C, Dabiri and Nilfouroushan (2024)/B,C,O, Torre et al. (2024), Lau et al. (2024)/C,O, Eskandari and Scaioni (2024)/O, Cuervas-Mons et al. (2024)/C,O, Parenti et al. (2024)/C, Cappadonia et al. (2024)/C,O, Lau et al. (2024)/O, Ghaderpour et al. (2024c)/C, Rudolf et al. (2024)/O, Bonasera et al. (2024)/O, Solarte et al. (2024)
Landslide inventories	Necula and Niculită (2023)/C, Necula and Niculită (2024)/C, Guinau et al. (2024)/C, Medici et al. (2024)/C, Antonielli et al. (2024)
Wide-area deformation studies	Palamà et al. (2024)/B, Cuevas-González (2026)/B, Crosetto et al. (2025)/B, Medici et al. (2025), Danezis et al. (2024), Magnall et al. (2024)
Geodynamics and tectonics	Atanasova and Nikolov (2023), Metzger et al. (2023)/O, Mildon et al. (2024)/O, Melichar et al. (2024)/O, Matano et al. (2024)/O, Bignami et al. (2024)/O
Underground mining	Pawłuszek-Filipiak et al. (2023)/O, Ilieva et al. (2024)
Open pit mining	Motagh et al. (2024), Tzampoglou and Loupasakis (2023)/O
Abandoned mines	Yang et al. (2023)/O, Tinagli et al. (2024)/O, Guzy (2024)/O
Infrastructures: bridges	Tonelli et al. (2023)/O, Eskandari and Scaioni (2023)/C,O, Evers et al. (2024), Simeone et al. (2024)/C, Coccimiglio et al. (2024)/O
Infrastructures: dams	Ruiz-Armenteros et al. (2023), Costantini et al. (2022)/B,C,O, Ruiz-Armenteros et al. (2024)/B,C
Civil infrastructure	Milenova Vasileva (2023)/O, Zêzere et al. (2024), Wang (2023)/O, Siegmund et al. (2024), Malinowska et al. (2024)/C, Sánchez-Fernández et al. (2024), Petio et al. (2024)
Infrastructures: gas storage	Fibbi et al. (2023)/C,O, Fibbi et al. (2024)/O, Rigamonti et al. (2024)
Infrastructures: landfills	Negula et al. (2023)/O
Urban areas and buildings	Mele et al. (2023)/C, Hlaváčová et al. (2023)/C,O, Shahbazi et al. (2024)/C, Rodríguez-Antuñano et al. (2023), Lenardón Sánchez et al. (2024)
Archaeology and cultural heritage	Antonioli et al. (2023)/O, Agapiou et al. (2023)/O, Ioannidis et al. (2024)/O, Lodigiani et al. (2024)/C, Tondi et al. (2024), Nikolov et al. (2023), Rodríguez-Antuñano et al. (2024), Chalkidou et al. (2024)/O
Miscellaneous	Pirotti et al. (2024)/O

two datasets. A correlation coefficient of 99% was obtained with an RMS difference of 1.4 mm/yr. This indicates the good quality of the EGMS Calibrated product for the retrieval of land subsidence rate maps and risk analysis in the region.

5.2. Tectonic features in the Mount Etna volcanic area

The DInSAR technique has been widely applied to monitor Mount Etna since the 90s, e.g. see Lanari et al. (1998) and Borgia et al. (2000). In this paper, we use EGMS data to study the ground motion astride part of the Pernicana fault i.e. the about E–W trending 18-km-long tectonic structure accommodating with left-lateral and normal components the seaward sliding of the volcano's eastern flank. The objective is to show the EGMS capability to capture differential ground motion between areas separated by this fault. Here we analyse the horizontal East/West and vertical Ortho products. Fig. 4 shows the horizontal East/West displacement of two areas located on two opposite sides of the Pernicana fault system. The Southern area shows a motion towards East up to 110 mm, with a mean velocity of about 16 mm/yr in the observed period, while the Northern area is basically stable. This agrees with previous studies, e.g. Rasà et al. (1996); Azzaro et al. (1998); Tibaldi and Groppelli (2002); Lundgren et al. (2004); Ruch et al. (2013); Pezzo et al. (2023). In the Vertical data (Fig. 4), the Southern area shows a general lowering trend, up to 35 mm in the observed 5 years, while to the Northern area is basically stable. This confirms the transtensive tectonics (extensional component added to the along-strike slip) of the Pernicana fault. The lowering trend of the Southern area can be associated to a decompression phase of the volcano that is also shown by the area north of the fault, starting at least since February 2020. The detected vertical slip rate results lower than the short-term throw rate of 10 mm/yr estimated by Azzaro et al. (2013) and the 15 mm/yr estimated by D'Amato et al. (2017) for the last 3.5 kyr. The time series show also evidences related to specific eruptive episodes. In fact, it is possible to distinguish, among others, the inflections corresponding to the volcanic activity started on December 4, 2021, on November 27, 2022, and on February 7, 2023. In the East-West time series, these dates correspond to accelerations, particularly in the area north of the Pernicana fault, while in the Vertical time series they correspond to evident subsidence.

5.3. Moving Area Clustering for Italy

This study has been based on the Ortho product of the 2019–2023 period, covering the Italian territory. Data have been downloaded using EGMSstream (Festa and Del Soldato, 2023) to pinpoint areas of active deformation (MAC, Moving Area Clustering), associating them different potential types of deformational processes. The procedure (Festa et al., 2022) consisted of three main steps: (i) filtering and spatial clustering to identify the most active areas; (ii) automatically determining the magnitude and the style of deformation; (iii) obtaining a preliminary interference of the underlying processes that triggered the detected areas affected by deformation.

Stable MPs were filtered out by adopting a stability threshold of ±1 cm/yr (Barra et al., 2017; Solari et al., 2019; Festa et al., 2022). The spatial MAC clustering was performed by adopting a buffer size of 100 m and fixing a minimum number of 3 contiguous MPs. For each MAC a set of morphometric parameters was calculated. A K_{VK} parameter, expressed as the ratio between the vertical and horizontal motion and describing the prevailing direction of the areal movement, was associated to every MAC. Finally, a categorization of each MAC into potential deformation processes has been performed, using a decision tree based on the outputs derived from (*i*) and (*ii*), as well as on the spatial correlation between the active motion areas and the pre-existing inventories and ancillary maps.

A total number of 65,704 MPs were selected to cover Italy, which resulted into 2475 MACs (Fig. 5), covering an area of 1.882 km^2. Potential triggering factors were sorted in 9 classes: landslide, potential landslide, subsidence, potential subsidence, dump, mining, deformation related to volcanic, uplift and potential uplift. A further category, i.e., unclassified, was used for those MAC falling outside the classification criteria. The distribution of MACs indicates that 54% of the total are landslides, 18% are ascribed to subsidence, less than 1% to volcanic activities, about 2% can be related to human activities (35 to mining and 21 to dump). 13% of MACs remain unclassifiable.

Deformations correlated to volcanic-type phenomena near Etna and Campi Flegrei, despite their low numerosity, cover a considerable areal

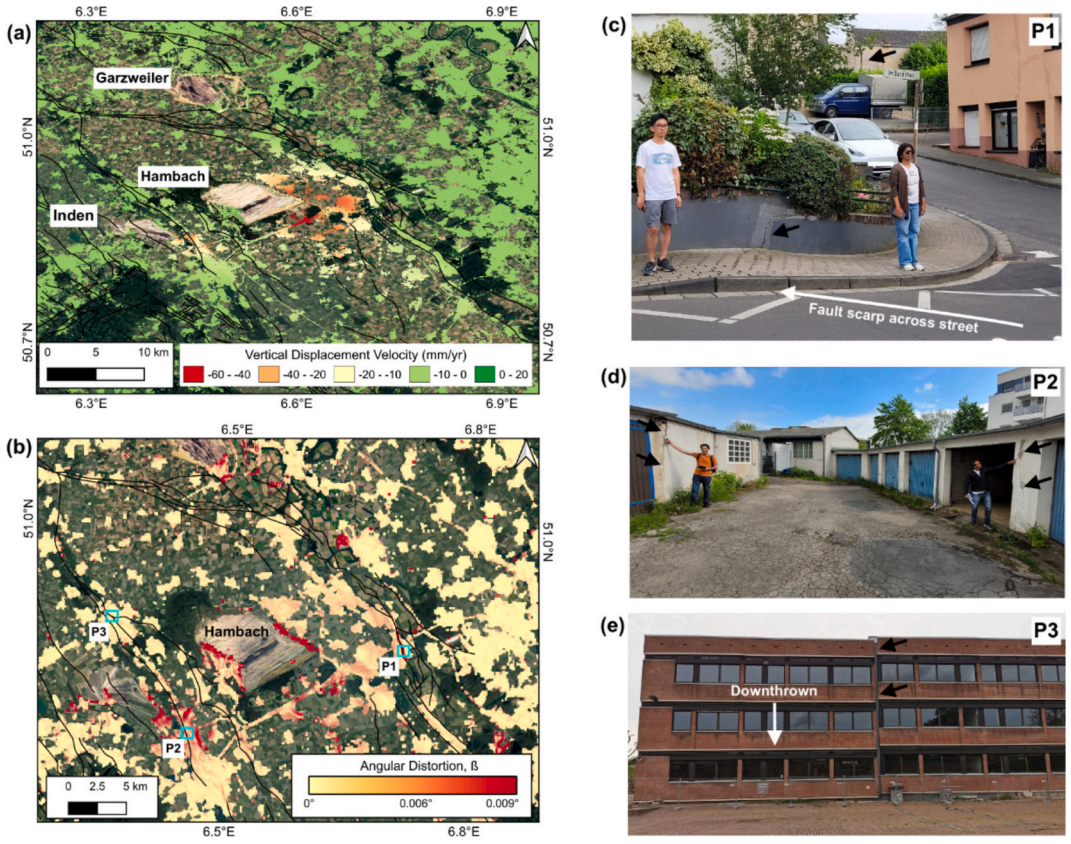

Fig. 2. (a) Vertical displacement rates from the Ortho EGMS product. (b) Angular distortion. (c-e) Examples of structural damage, marked by black arrows, at locations labeled in (b) with P1, P2 and P3, respectively. (c) A fault step and damage to private houses in Horrem (Photo credit: Mahdi Motagh, June 2024). (d) Structural damage to an abandoned garage in Düren (Photo credit: Mahdi Motagh, May 2023). (e) Damage to a school in Jülich due to differential displacement, causing a clear offset in the row of windows in the middle of the school (Photo credit: Mahdi Motagh, May 2021).

extension. The clusters classified as landslides are notable for their extensive areal diffusion. They are numerous, extending along the entire Apennine arc with a pronounced concentration in the Northern and Southern Apennines. Finally, subsidence deformations are present in the major Italian plains, with a particular prevalence in the Po Valley and internal flat areas.

This study applied simple tools for the analysis of ground deformation maps provided by InSAR processing at national scale, which may contain millions of MPs. Dealing with such large amount of data, PSI manual analysis and interpretation is no longer an option. The need for implementing efficient value-adding tools able to optimise InSAR data usage is urgent. We believe that two common goals should be pursued by the communities of end users and researchers in order to maximize the value-added products from the increasing availability of interferometric results and to solve the bottleneck currently represented by the limited capability in data analysis and interpretation: *i*) refinement and automatization of existing tools to transform InSAR data and geological knowledge into usable information to be ingested within policies to reduce the hazards and *ii*) definition of standardized methodologies, best practice for data analysis, criteria for ensuring transferability and facilitating homogenous products.

5.4. Analysis of ground deformation along England and Wales coastlines

More than 5.3 M residents live nearby the ~9000 km of coastlines of England and Wales (ONS, 2020). These areas are threatened by multiple hazards (Sea Level Rise - SLR, coastal erosion and flooding) that can result in severe socio-economic impacts and will be further exacerbated by climate-change (Barnard et al., 2024). For this case study, we applied a novel Machine Learning approach to automatically analyse the main patterns of the EGMS Ortho product along the coastline of England and Wales.

We used a Seasonal Trend Linear-decomposition and Piecewise Linear Regression (STL-PLR) tool developed at the British Geological Survey (Hourston et al., 2024). This tool decomposes EGMS time series into a general segmented trend, its seasonal component, and residual signals (Fig. 6), by first applying the STL to extract the trend and seasonality components of the signal. Then, a PLR is used to fit the trend with a variable number of linear segments, depending on the trends in the displacement time series. This allows us to expand beyond merely distinguishing between uplifting, subsiding or stable indicators. Indeed, by using the STL-PLR we are able to define a new category of "non-linear" moving points.

Additionally, for these points we are also able to automatically identify breakpoints at which time the motion pattern changes, either by accelerating or decelerating. The stable category is determined by a deformation velocity threshold, which corresponds to 1.5σ, where σ is the standard deviation of the deformation rate of the UK's coastlines. Any InSAR point moving at a rate within plus or minus of this number is assigned "linear-stable". The variable number of linear segments used in the PLR is determined by gradually increasing the number of segments and comparing the resulting adjusted R^2 coefficient of both models. If the increase in the new model's adjusted R^2 is larger than 3%, then the more complex model is accepted, and again a new segment is added. This process continues until this increase in adjusted R^2 becomes equal to or smaller than 3%. We have defined four classes: linear-stable, linear-uplift, linear-subsiding, and non-linear.

We analyzed the vertical deformation of the Ortho 2018–2022 product. To enable better decision-making for coastal managers, who are typically interested in spatially broad patterns of motion, we needed

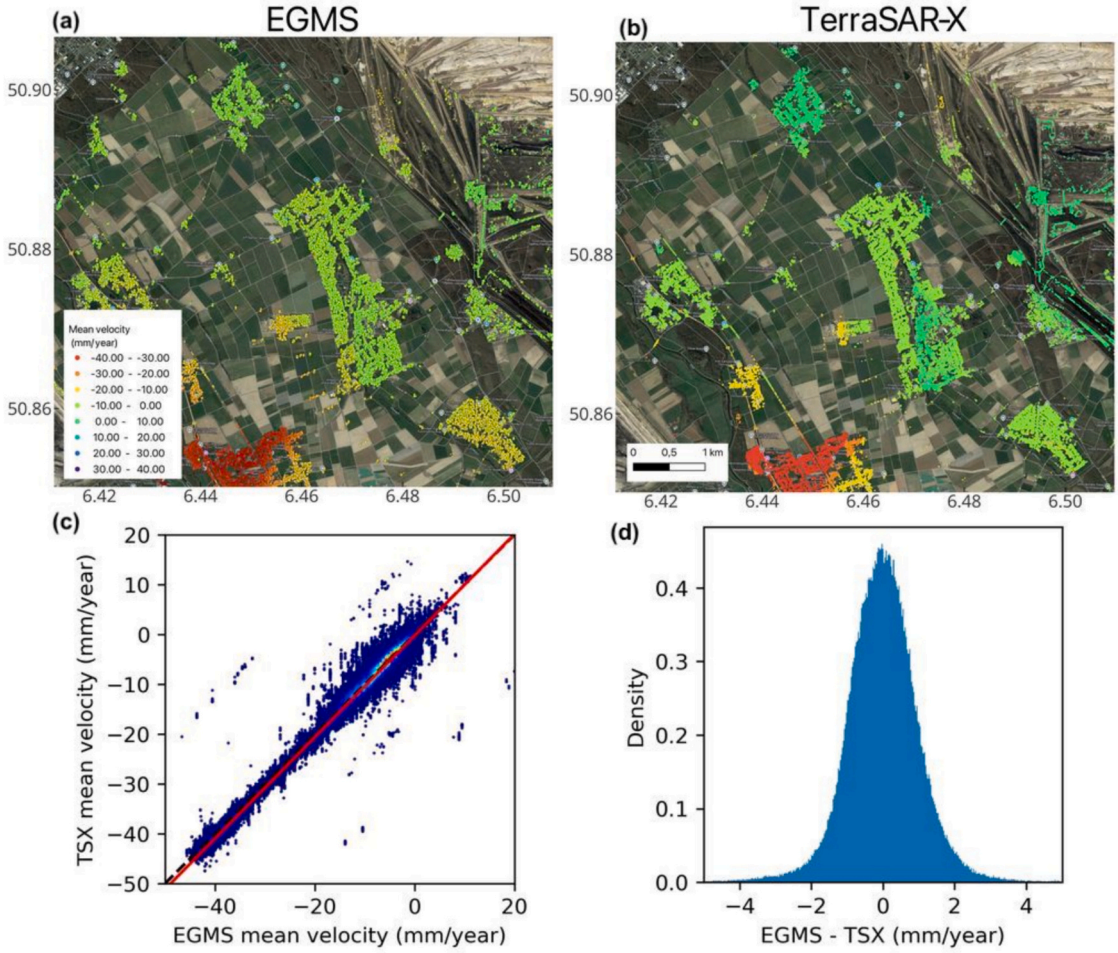

Fig. 3. (a) Line-of-sight displacement rates from the EGMS Calibrated product (a) and TerraSAR-X (TSX) (b). The average TSX density is 5000 MP/km^2, while the EGMS density is 600 MP/km^2. Correlation (c) and histogram of differences (d) between EGMS and TSX.

to spatially and visually simplify these measurements. We assigned each Ortho pixel with an elevation according to the NEXTMap British Digital Elevation Model (Intermap Technologies, 2007) at 50-m resolution. We extracted all pixels located at elevations ≤10 m, which predominantly reflect coastal lowland areas. We produced a 1x1km grid over the UK and determined the modal deformation behaviour of all pixels within each grid (Fig. 7). Our tool then enables plotting simplified barycentre (median and mean) time series of all pixels within each of the grids (Fig. 7). We finally compared the predominant motion pattern with both the bedrock and superficial geology from the BGS Geology dataset (https://www.bgs.ac.uk/datasets/bgs-geology-50k-digmapgb/) to support interpretation of the potential source of ground motion observed over large areas.

Our results show that 13.9% (2243 km^2) of the coastal region in the south and east of England exhibit predominantly linear-subsidence deformation behaviour, 47.5% (7659 km^2) is stable and 0.2% (36 km^2) show linear-uplift behaviour. The dominant deformation pattern is non-linear with 38.4% (6188 km^2) of the coastland lowland areas showing this behaviour in the time series.

We observe a good spatial corelation with the superficial geology; subsidence (linear and non-linear) dominates in areas of thick superficial peats, clays and silts such as the alluvium along the Thames Estuary and the Fens area north of Cambridge. Areas predominantly composed of superficial sands and gravels show greater stability. Within the subsidising areas the identification of non-linear behaviour is key to understanding the timing of subsidence change which helps make the link to the underlying process and hence enables a consideration of how the process might change in response to climate change.

Coastal vertical land motion, and subsidence in particular, represent a major threat for the coastlines of England and Wales with velocity rates up to −30/−40 mm/yr in some areas, which is more than two times the rate of SLR expected in this area by 2100 (IPCC, 2021). Identifying and characterising such motion along the coast now is a key aspect to mitigate the impact of natural hazards in the future. The ML tools developed allows us to better analyse relationship between geology (superficial vs. bedrock and anthropogenic deposits/factors) and ground stability conditions with a particular focus on identifying the causes of non-linear motions and the acceleration or deceleration observed in time series.

5.5. *Analysis of differential ground deformation in Spain*

In this case study, we focus the attention on spatial differential deformations or spatial gradient values, which are directly related to damages to buildings and infrastructures. We used the procedure described in Shahbazi et al. (2024), to derive the so-called Building Differential Deformation (BDD) map. The procedure requires as inputs the EGMS Basic product and a vector map of buildings and infrastructures. For all buildings and infrastructures covered by enough MPs, the procedure computes the gradient of the deformation field, keeping for each building its maximum value. Each building is assigned a gradient class. It is important to underline that procedure reliability depends on the number of MPs falling inside a given building. Shahbazi et al. (2024) indicate a minimum number of 15 MPs per building to

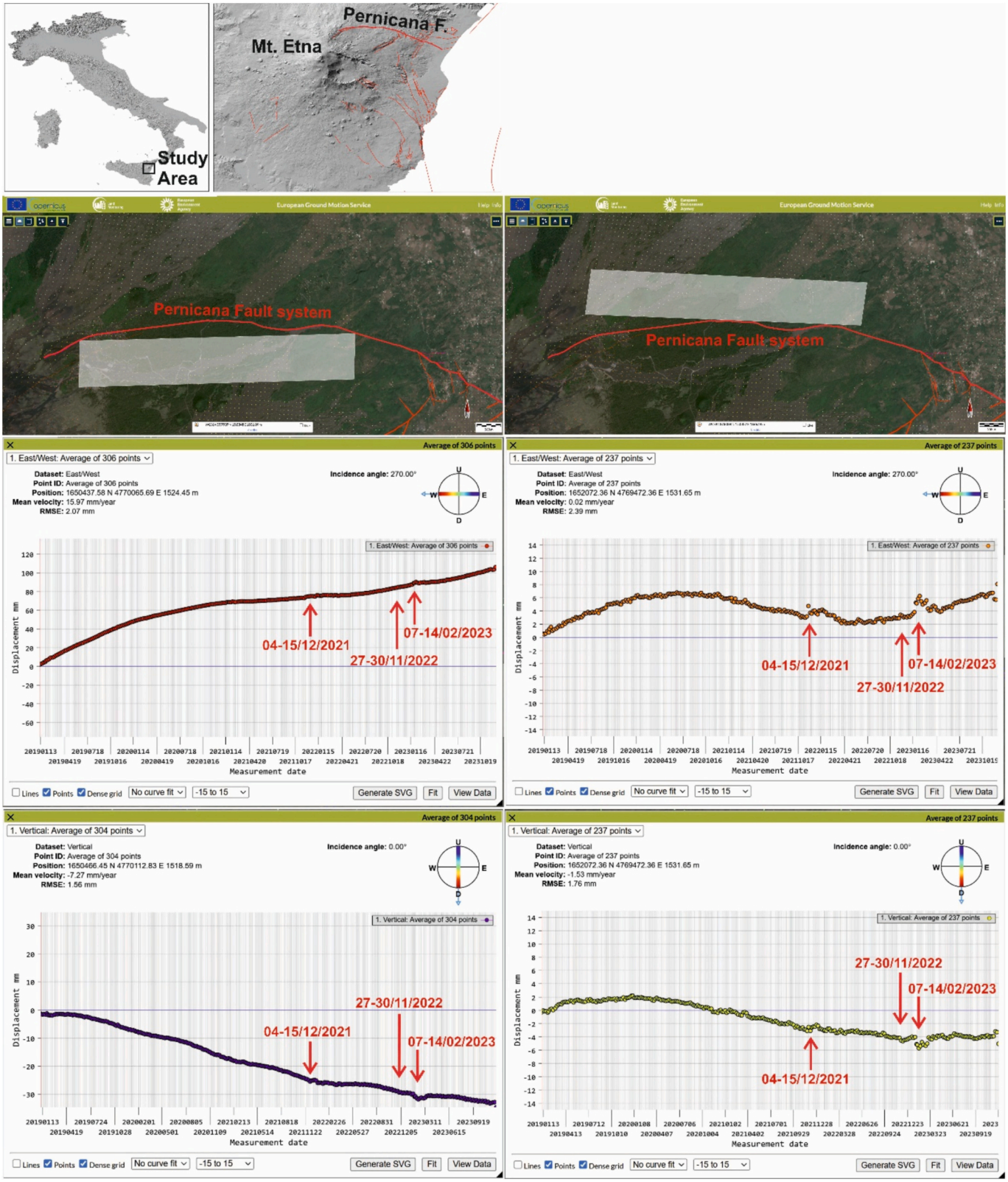

Fig. 4. Location of the investigated Southern and Northern areas (upper-left and upper-right). Polygons are about 1 by 6.5 km.; East-West horizontal displacement of the Southern area (middle-left); East-West horizontal displacement of the Northern area (middle-right); Vertical displacements of the Southern area (bottom-left); Vertical displacements of the Northern area (bottom-right). Faults are from the ITHACA Catalogue (https://sgi.isprambiente.it/ithaca/viewer/index.html). The DEM is from TINITALY (Tarquini et al., 2023).

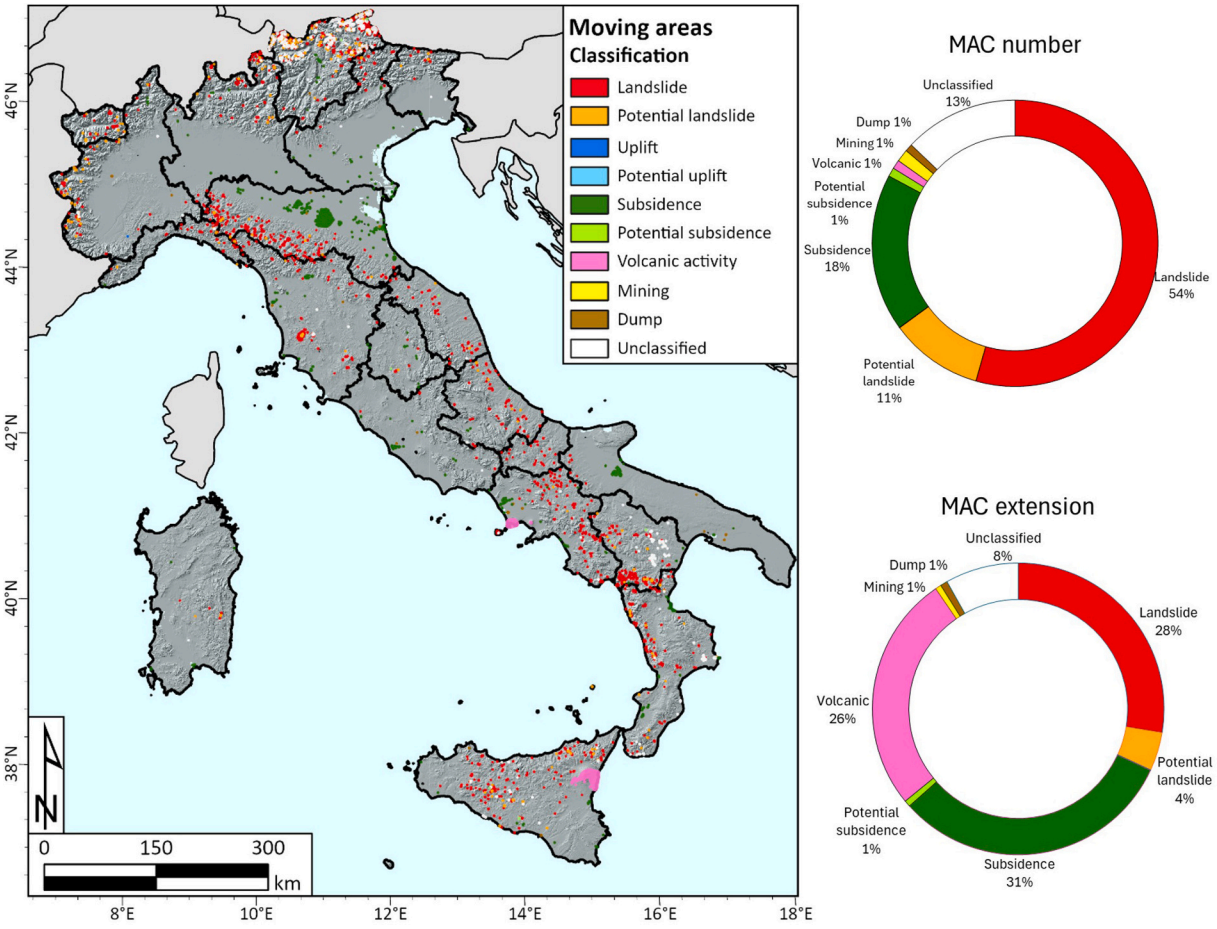

Fig. 5. MP mapping results for the Italian territory. In the inset percentages of MAC, in terms of number and extension, are reported.

achieve a reliable gradient estimation.

The BDD can be a useful screening tool to analyse large PSI datasets. In this study the analysis covered the entire territory of Spain. Input were the EGMS basic products in ascending geometry over Spain mainland, and the vector map of buildings from OpenStreetMap (www.openstreetmap.org). Due to a lack of data in certain locations, particularly in southern Spain, we added another layer known as Cadastral Inspire data of Spain. Fig. 8 illustrates the inputs and outputs of the procedure. A total of 2958 buildings were identified, which suffer absolute deformation gradient values above 0.05 mm $\times$ yr^{-1} $\times$ m^{-1}. It is important to note that all the identified buildings are large and typically located in industrial areas. This is due to the constraint of a minimum of 15 MPS per building. 20% of the identified buildings fall in the Very Low gradient intensity class; 36% in the Low class, 24% in the Medium, and the remaining in the High intensity class. For several buildings, validation activities have been carried out (Shahbazi et al., 2024).

The BDD map is a useful tool for identifying at-risk buildings over wide areas. For instance, it can be used as an entry level screening to drive a more detailed building-wise analysis. A further evolution is the estimation of impact, which takes into account the deformation velocity, the age of construction and the affected population, see Shahbazi et al. (2025).

6. EGMS evolution

Considering the experience gained in the last years, it is interesting to consider the potential future evolution of EGMS. Our vision is described below.

- **Going global: a stepwise extension of EGMS towards global coverage.** A Copernicus Global Ground Motion Service (CGGMS) could be introduced, consisting of the most quality-controlled InSAR based ground motion dataset worldwide. CGGMS would be a major contribution from Europe to the Sendai Framework for Disaster Risk Reduction, especially for understanding disaster risk (Priority 1) and investing in disaster risk reduction for resilience (Priority 3). A CGGMS would have global use with respect to: identifying landslide risk areas, reducing disaster risk, identifying coastal areas with land subsidence thus improving climate adaptation to future sea level rise, improving monitoring of geodynamics and tectonics and mining activities, improving infrastructure planning in areas with subsidence through monitoring of infrastructure subsidence, instability and vulnerability, and monitoring of subsidence due to exploitation of aquifers and thus improving monitoring and sustainability of ground water world-wide.
- **The geographic extension** from EGMS to CGGMS could first involve the following steps:
  - o Extension of the current European coverage to EEA39 including Jan Mayen, Liechtenstein, Switzerland, Turkey, Albania, Bosnia and Herzegovina, North Macedonia, Montenegro, Serbia and Kosovo from 2028.
  - o Extension of EGMS to Ukraine.
  - o Extension of EGMS to cover polar/high altitude areas with permafrost, see earlier work in Rouyet et al. (2019). It was stated in the Copernicus polar roadmap for service evolution (Duchossois et al., 2024) that EGMS should be expanded to a pan-Arctic scale to provide ground motion information on the ongoing thawing of permafrost and implications for the environment and

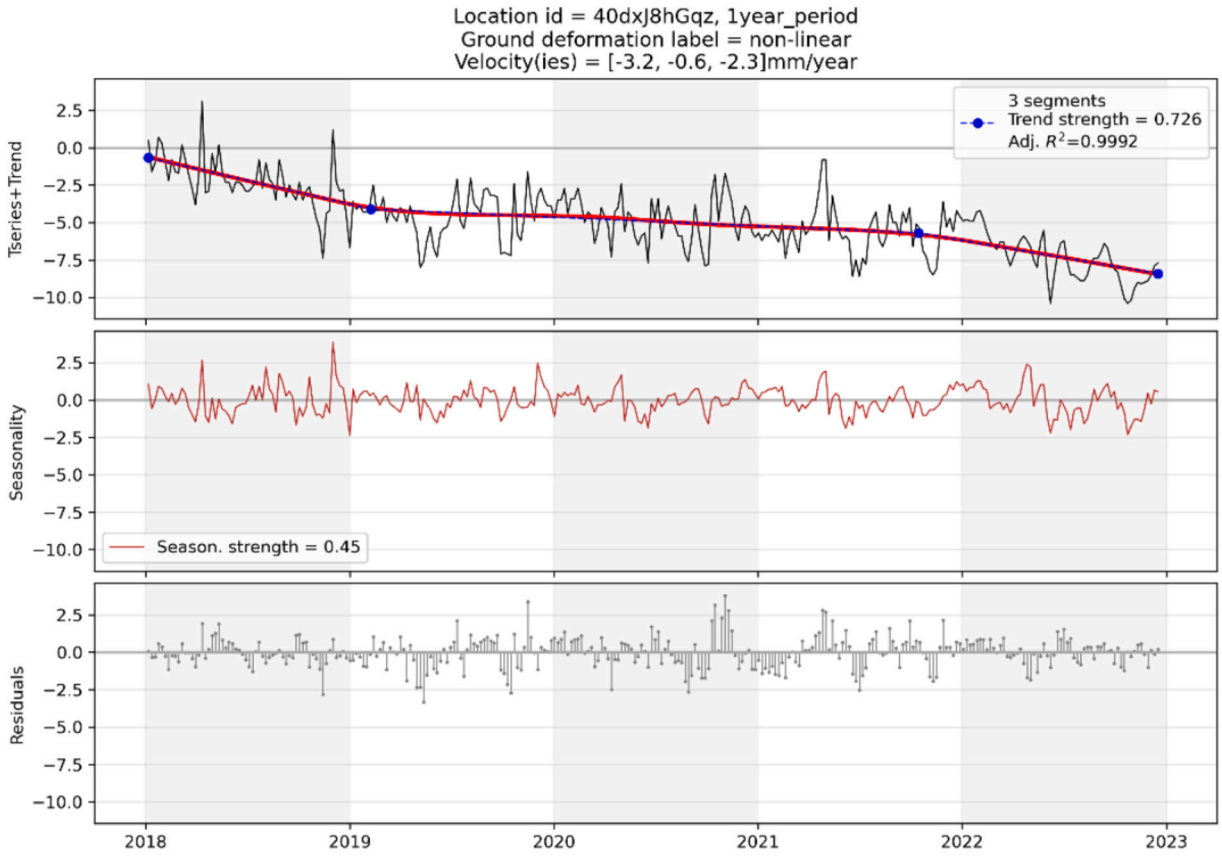

Fig. 6. An example of a seasonally decomposed InSAR timeseries from southeast England, demonstrating a non-linearly behaving ground deformation pattern. The velocities listed in the title correspond to the three segments determined by the STL-PLR algorithm.

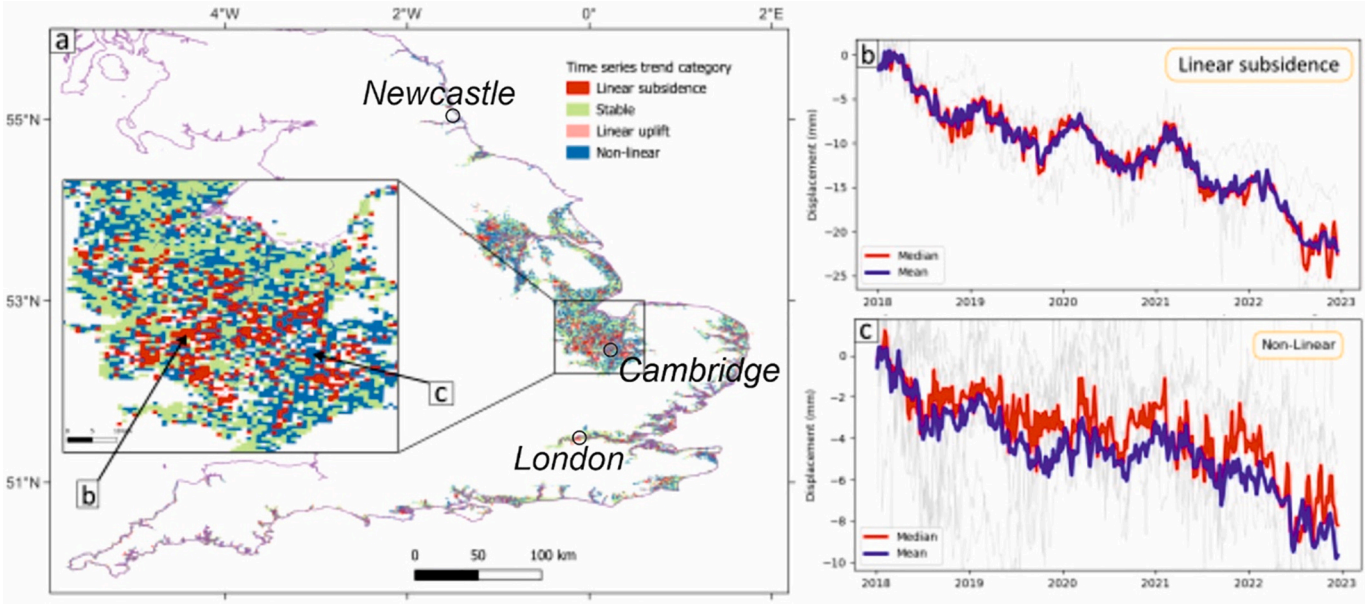

Fig. 7. a) Deformation time series trends across coastal lowland areas around south and east England. Examples of barycentre time series for selected points indicated in the inset on figure (a) for linear subsidence (b) and non-linear motion (c). Grey lines are the individual pixel time series while the red and blue are the barycentre median and mean respectively. (For interpretation of the references to colour in this figure legend, the reader is referred to the web version of this article.)

infrastructure. This can be extended from InSAR Svalbard to include seasonal coverage of ice-free parts with permafrost on Svalbard, Arctic islands and Greenland from 2028. Ice free parts of Antarctica, Antarctic islands and other high mountainous parts of the world with permafrost could potentially be covered from 2031.

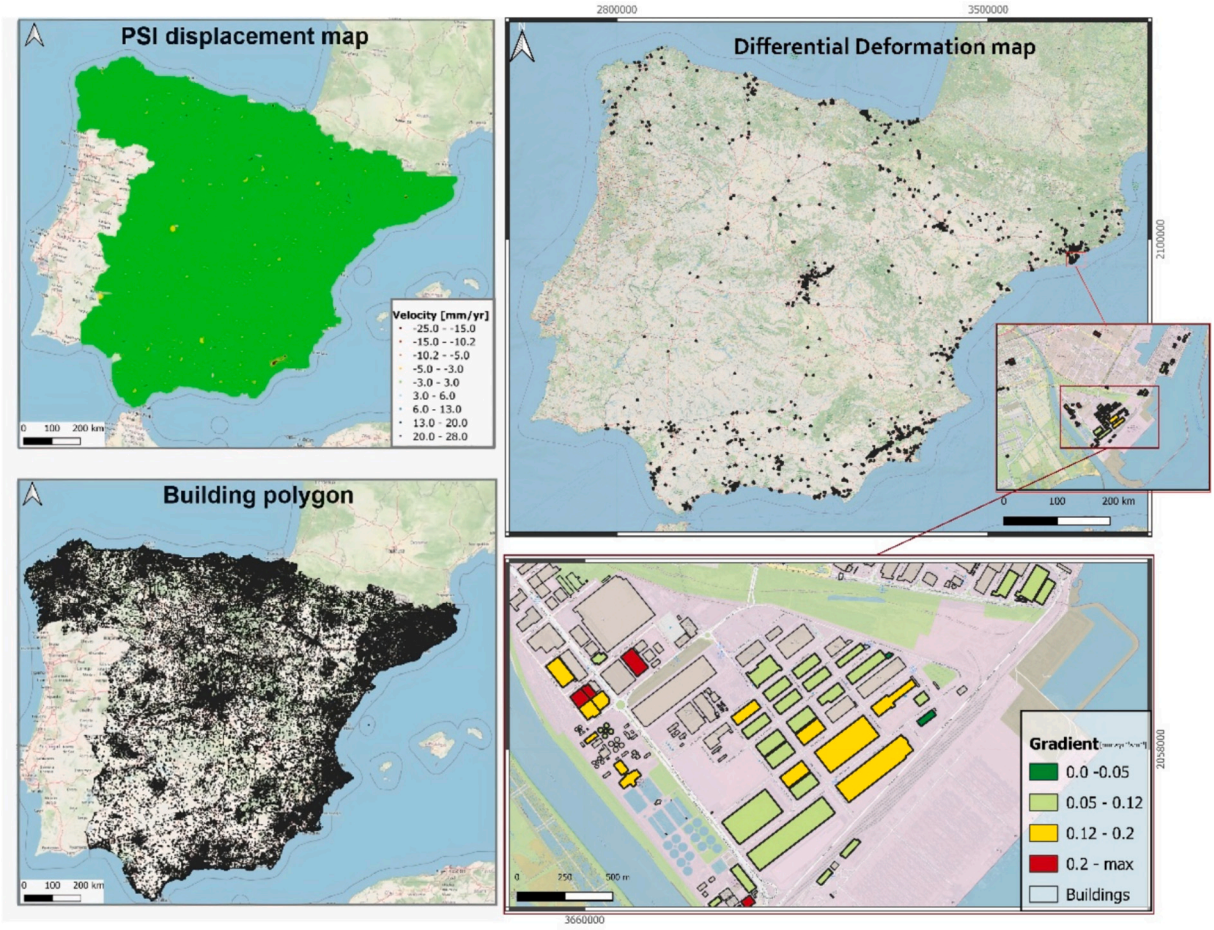

Fig. 8. Deformation velocity map (upper-left), building polygons (bottom-left), Building Differential Deformation (BDD) map (upper-right) and zoom over an industrial area of Barcelona.

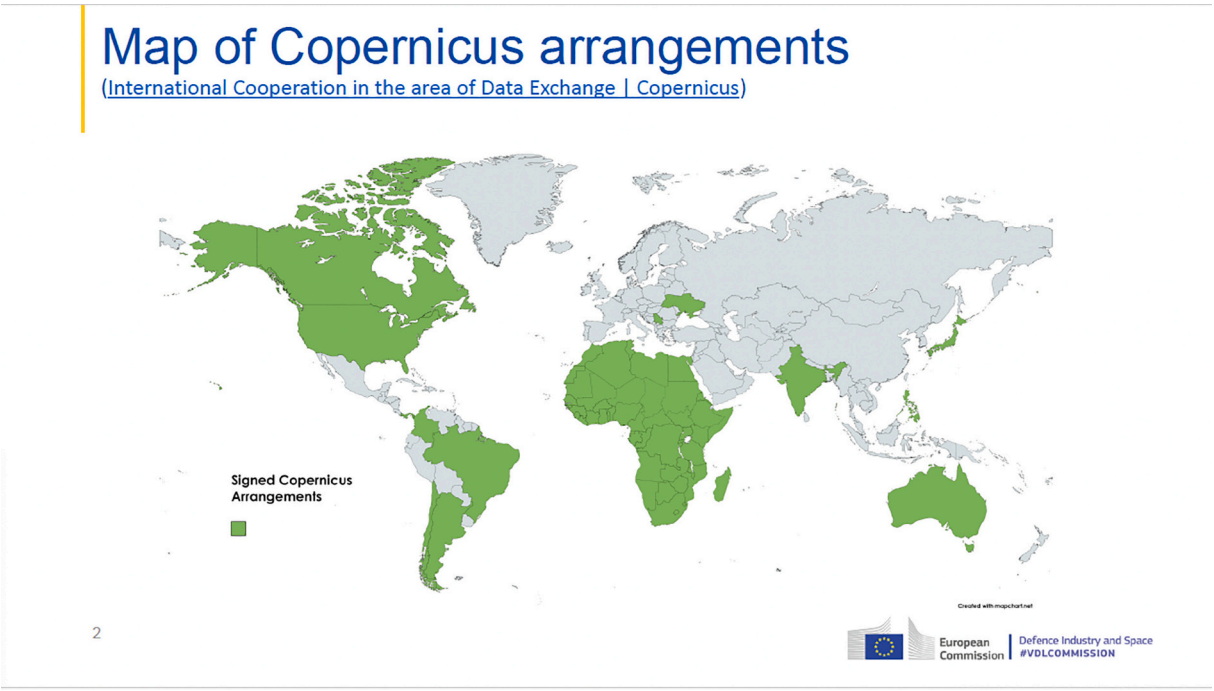

Fig. 9. Map of the Copernicus Collaboration Agreements.

  - o Extension of EGMS to cover remaining overseas regions islands and territories of France, Spain, Netherlands, Portugal and United Kingdom, including French Guiana.
- **Priorities outside Europe** are suggested to be given to nations and/or continents with Copernicus Collaboration Agreements (see Fig. 9) that can supply relevant in-situ data and GNSS models and collaborate on the development of a quality controlled CGGMS. A stepwise approach is suggested starting from:
  - o Australia with future extensions to New Zealand and Oceania.
  - o South America with first priority on Chile, Argentina, Brazil, Colombia and Panama exploiting collaboration with regional Copernicus Centres in Panama and Chile.
  - o South-East Asia with first priority on India, Philippines (Collaboration with the Bilateral Copernicus Centre in the Philippines), Singapore, Vietnam, Thailand, Indonesia, South Korea, Nepal and Himalaya.
  - o Africa exploiting collaborations between the European Commission, the African Union, ESA, EEA and the newly started African Space Agency and the EU-Africa Space cooperation flagship.
  - o Canada potentially through combined use with Radarsat Constellation Mission data.
  - o Japan potentially through collaborations with JAXA on combined use of ALOS data.
  - o United States potentially through collaboration with NASA and USGS.
  - o Remaining parts of Eastern Europe and Asia including China, Russia and Middle East.

Towards the implementation of CGGMS, it is suggested to write a white paper in order to further detail the specification and potential of CGGMS including potentially having a series of workshops with relevant stakeholders from potential CGGMS collaboration partners from different countries and continents.

- **Extend EGMS with L-band InSAR**. Sentinel ROSE-L will be launched in 2028, and L-band InSAR from ROSE-L can be integrated in EGMS from 2029/2030. NASA/ISRO NISAR, launched in 2025, can earliest be integrated in EGMS from 2028. L-band InSAR have an extensive potential for ground motion and will be able to measure larger deformations than S-1 due to the longer wavelengths of L-band (23–24 cm) relative to C-band (5.6 cm). L-band will also improve InSAR measurements over forest, thus giving a higher point density for EGMS. Finally, L-band InSAR has historically been better to use over permafrost, being able to measure decadal subsidence in addition to seasonal subsidence (Rouyet et al., 2019, 2024).
- **Integration of S-1 Next Generation in EGMS**. S-1 NG will earliest be launched in 2032 and can earliest be phased into EGMS by the end of 2033 or 2034. A decrease of the temporal baseline of the SAR acquisitions will allow to solve faster ground motion phenomena, overcoming the current limit of ~2 mm/day. Enhanced resolution will entail a better definition of radar stable ground targets and an improvement of the number of MPs per unit area.
- **Research and development in support of future EGMS needs.** In order to continue to develop the state-of-the-art European InSAR competence cluster, research should include:
  - o 3D InSAR from the ESA Earth Explorer bistatic radar mission Harmony (flying together with S-1) and studies into the potential impact on further development of 3D InSAR and the Ortho product in EGMS.
  - o High temporal emergency use of InSAR with e.g. ICEYE.
  - o The IRIDE NIMBUS SAR low inclination mission for better understanding of InSAR of north/south slopes with potential impact for improving the EGMS Ortho product in Southern part of Europe.
- **Integration of big data analytics tools in EGMS.** Integration of some new big data analytics tools should be done in the EGMS WebGIS for example for automatic extraction of ADAs. Development of a federated ecosystem of big data analytics tools for EGMS can potentially be stimulated.
- **Application of EGMS in relevant EU regulations.** A feasibility study should be performed with respect to future potential inclusion of application of EGMS related findings in EU regulations for e.g. disaster risk, climate adaptation, water management, infrastructure maintenance, urban planning and mining.

7. Conclusions

In this paper the EGMS has been described, and its impact has been investigated. The main technical aspects involved in the service have been outlined. An entire section has been devoted to EGMS user uptake, considering data download, scientific literature, and the usage beyond the academic domain. The increasing number of publications and data downloads indicate a growing recognition of EGMS as a valuable tool for understanding ground deformation processes and their source. The published studies demonstrate the wide-ranging utility of EGMS data across various applications, extending beyond academic research to practical infrastructure monitoring and hazard mitigation so benefitting also public bodies and private companies. There is an increasing trend of integrating InSAR data with Artificial Intelligence/ Machine Learning tools. The development of these tools will further facilitate the uptake of the EGMS data over large scale and prediction scenarios for ground deformation.

An important section of the paper has been devoted to the discussion of five key applications, to illustrate the EGMS potential. Two studies concern local areas: mining-induced deformation and the study of tectonic features in the Mount Etna area. The last three studies involve wide-area EGMS data and EGMS analyses on national scale, with the potential to be extended to the entire continent. The first one includes the clustering of moving areas for Italy, the second one the analysis of ground deformation along England and Wales coastlines, and the third one the analysis of differential ground deformation in Spain.

In the last part of the paper, the potential evolution of EGMS has been addressed. This includes a stepwise extension of EGMS towards global coverage, creating the Copernicus Global Ground Motion Service (CGGMS). This would represent a major contribution from Europe to the Sendai Framework for Disaster Risk Reduction. A roadmap for extension from EGMS to CGGMS has been outlined, starting from Europe up to reaching a global coverage. Additionally, the use of L-band data from ROSE-L and NISAR has been mentioned, as well as the use of S-1 Next Generation data. The last part of this section has included a short list of research and development in support of future EGMS needs, the need to integrate new big data analytics tools in the EGMS WebGIS, and the effort needed to foster the inclusion of application of EGMS related findings in EU regulations.

CRediT authorship contribution statement

M. Crosetto: Writing – review & editing, Writing – original draft, Supervision, Methodology, Conceptualization. **M. Cuevas-González:** Methodology, Conceptualization. **M. Mróz:** Methodology, Conceptualization. **D.A. Moldestad:** Writing – review & editing, Methodology. **F. Raspini:** Writing – review & editing, Investigation. **N. Casagli:** Investigation. **L. Bateson:** Investigation. **A. Novellino:** Writing – review & editing, Investigation. **M. Motagh:** Writing – review & editing, Investigation. **L. Guerrieri:** Writing – review & editing, Investigation. **V. Comerci:** Writing – review & editing, Investigation.

Declaration of competing interest

We state that there is no financial or personal interest or belief that could affect our objectivity.

Acknowledgements

This work is part of the Spanish Grant SARAI, PID2020-116540RB-C21, funded by MCIN/AEI/ 10.13039/501100011033. This work has also been partially funded by the European Environment Agency through the project "Copernicus European Ground Motion Service—Supporting Services" (Contract EEA/DIS/R0/22/004). The authors thank Lorenzo Solari from the European Environment Agency for providing the data relative to the EGMS downloads. The authors would like to thank E. Hussain and H. Hourston from the British Geological Survey (UK) for their key contribution to Section 5.4 on the analysis of ground deformation along England and Wales coastlines. TerraSAR-X data used in Fig. 3 are copyright of German Aerospace Agency (DLR) and were provided via proposal motagh_GEO1916. Field surveys in the Rhineland Coalfield area were performed within the framework of the project "SARKI4Tagebaufolgen" financed by the Bundesministerium für Wirtschaft und Energie (BMWE) in Germany.

Data availability

Data will be made available on request.

References

Adamski, M., et al., 2024. Efekt rzeczowy z realizacji przedsięwzięcia z zakresu państwowej służby geologicznej (in Polish). https://www.pgi.gov.pl/images/monitoring-osiadan/raport_1.pdf.

Agapiou, A., Kyriakidis, P., Hadjipetrou, S., Kyriakides, N., Votsis, R., 2023. European ground motion service for built heritage: a case study from Cyprus. In: International Symposium on Digital Earth.

Antoniadis, N., Alatza, S., Loupasakis, C., Kontoes, C., 2023. Land subsidence phenomena vs. coastal flood hazard—the cases of Messolonghi and Aitolikon (Greece). Remote Sens. 15 (8), 2112.

Antonielli, B., Caprari, P., Marmoni, G.M., Marini, R., Di Renzo, M.E., Giordano, A., et al., 2024. Landslide monitoring at both large and detailed scales using satellite A-DInSAR in southern Lazio (Italy). Italian J. Eng. Geol. Environ. 5–14.

Antonioli, F., Furlani, S., Spada, G., Melini, D., Zomeni, Z., 2023. The Lambousa (Cyprus) fishtank in a quasi-stable coastal area of the eastern Mediterranean, a notable marker for testing GIA models. Geosciences 13 (9), 280.

Atanasova, M., Nikolov, H., 2023. Application of SAR data time series for monitoring of geodynamic processes in the Sofia region. Int. Multidiscip. Sci. GeoConf.: SGEM 23 (2.1), 283–290.

Azzaro, R., Ferreli, L., Michetti, A.M., et al., 1998. Environmental hazard of capable faults: the case of the Pernicana fault (Mt. Etna, Sicily). Nat. Hazards 17, 147–162. https://doi.org/10.1023/A:100803442208.

Azzaro, R., Bonforte, A., Branca, S., Guglielmino, F., 2013. Geometry and kinematics of the fault systems controlling the unstable flank of Mt. Etna volcano (Sicily). J. Volcanol. Geotherm. Res. 251, 5–15. https://doi.org/10.1016/j.jvolgeores.2012.10.001.

Barnard, P.L., Befus, K.M., Danielson, J.J., Engelstad, A.C., Erikson, L.H., et al., 2024. Projections of multiple climate-related coastal hazards for the US Southeast Atlantic. Nat. Clim. Chang. 1–9.

Barra, A., Solari, L., Béjar-Pizarro, M., Monserrat, O., Bianchini, S., Herrera, G., et al., 2017. A methodology to detect and update active deformation areas based on Sentinel-1 SAR images. Remote Sens. 9 (10), 1002.

Beccaro, L., Cianflone, G., Tolomei, C., 2023. InSAR-based detection of subsidence affecting infrastructures and urban areas in Emilia-Romagna region (Italy). Geosciences 13 (5), 138.

Berardino, P., Fornaro, G., Lanari, R., Sansosti, E., 2002. A new algorithm for surface deformation monitoring based on small baseline differential SAR interferograms. IEEE Trans. Geosci. Remote Sens. 40, 2375–2383. https://doi.org/10.1109/tgrs.2002.803792.

Bignami, C., Pignatelli, A., Romoli, G., Doglioni, C., 2024. Artificial-intelligence-based classification to unveil geodynamic processes in the eastern Alps. Remote Sens. 16 (23), 4364.

Bonasera, M., Taboni, B., Caselle, C., Acquaotta, F., Fubelli, G., Masciocco, L., et al., 2024. Instrumental monitoring of a slow-moving landslide in Piedmont (Northwest Italy) for the definition of rainfall thresholds. Sensors 24 (11), 3327.

Borgia, A., Lanari, R., Sansosti, E., Tesauro, M., Berardino, P., Fornaro, G., 2000. Actively growing anticlines beneath Catania from the distal motion of Mount Etna's decollement measured by SAR interferometry and GPS. Geophys. Res. Lett. 27 (20), 3409–3412.

Bru, G., Ezquerro, P., Béjar-Pizarro, M., Guardiola-Albert, C., Fernández-Merodo, J.A., Díaz, J.E.H., Herrera, G., 2024. InSAR-based assessment of land subsidence related to aquifer overexploitation in Spain: a comprehensive review. In: 2024 IEEE Mediterranean and Middle-East Geoscience and Remote Sensing Symposium, M2GARSS, pp. 386–390.

Capes, R., Passera, E., 2023. Product Description and Format Specification. EEA, p. 33. https://land.copernicus.eu/en/technical-library/egms-product-description-document/@@download/file.

Cappadonia, C., Confuorto, P., Di Martire, D., Calcaterra, D., Moretti, S., Rotigliano, E., Guerriero, L., 2024. Geomorphological insights to analyze the kinematics of a DSGSD in Western Sicily (southern Italy). Remote Sens. 16 (21), 4040.

Cappucci, S., Carillo, A., Iacono, R., Moretti, L., Palma, M., Righini, G., et al., 2024. Evolution of coastal environments under inundation scenarios using an oceanographic model and remote sensing data. Remote Sens. 16 (14), 2599.

Chalkidou, S., Georgiadis, C., Roustanis, T., Patias, P., 2024. A methodology for identifying coastal cultural heritage assets exposed to future sea level rise scenarios. Appl. Sci. 14 (16), 7210.

Cigna, F., Tapete, D., 2021. Satellite InSAR survey of structurally-controlled land subsidence due to groundwater exploitation in the Aguascalientes Valley, Mexico. Remote Sens. Environ. 254, 112254.

Cigna, F., Bonì, R., Teatini, P., Paranunzio, R., Zoccarato, C., 2024. Assessing current and future land subsidence risk induced by groundwater exploitation in Italy using earth observation. In: 2024 IEEE Mediterranean and Middle-East Geoscience and Remote Sensing Symposium, pp. 406–409.

CNR IRPI, 2024. https://www.irpi.cnr.it/project/dati-egms-negli-strumenti-di-pianificazione-pai.

Coccimiglio, S., Scussolini, L., Matteini, I., Ceravolo, R., Ferro, G.A., 2024. Interferometric satellite data for the structural health monitoring of infrastructures. Procedia Struct. Integrity 62, 840–847.

Costantini, M., Falco, S., Malvarosa, F., Minati, F., 2008. A new method for identification and analysis of persistent scatterers in series of SAR images. Proceedings of IGARSS 2008, Boston.

Costantini, M., Minati, F., Trillo, F., Ferretti, A., Passera, E., Rucci, A., et al., 2022. EGMS: Europe-wide ground motion monitoring based on full resolution InSAR processing of all Sentinel-1 acquisitions. In: IGARSS 2022, pp. 5093–5096.

Crosetto, M., Solari, L., 2023. Satellite Interferometry Data Interpretation and Exploitation: Case Studies from the European Ground Motion Service (EGMS). Elsevier.

Crosetto, M., Monserrat, O., Cuevas-González, M., Devanthéry, N., Crippa, B., 2016. Persistent Scatterer Interferometry: a review. ISPRS J. Photogramm. Remote Sens. 115, 78–89.

Crosetto, M., Solari, L., Mróz, M., Balasis-Levinsen, J., Casagli, N., Frei, M., Oyen, A., Moldestad, D.A., Bateson, L., Guerrieri, L., Comerci, V., Andersen, H.S., 2020. The evolution of wide-area DInSAR: from regional and national services to the European ground motion service. Remote Sens. 12 (12), 2043.

Crosetto, M., Crippa, B., Mróz, M., Cuevas-González, M., Shahbazi, S., 2025. Applications based on EGMS products: a review. Remote Sens. Appl.: Soc. Environ. 37, 101452.

Cuervas-Mons, J., Domínguez-Cuesta, M.J., Jiménez-Sánchez, M., 2024. Potential and limitations of the new European ground motion service in landslides at a local scale. Appl. Sci. 14 (17), 7796.

Cuevas-González, et al., 2026. Semi-automatic classification of unstable areas detected by the European ground motion service (EGMS) at national level. IEEE J. Sel. Top. Appl. Earth Obs. Remote Sens. (in press).

Dabiri, Z., Nilfouroushan, F., 2024. Enhancing landslide preparedness: leveraging EGMS products and SBAS-InSAR for pre-event ground deformation monitoring along the E6 highway near Stenungsund in southern Sweden. In: EGU General Assembly Conference Abstracts, EGU24-12802.

D'Amato, D., Pace, B., Di Nicola, L., Stuart, F.M., Visini, F., Azzaro, R., Branca, S., Barfod, D.N., 2017. Holocene slip rate variability along the Pernicana fault system (Mt. Etna, Italy): evidence from offset lava flows. GSA Bull. 129 (3–4), 304–317. https://doi.org/10.1130/B31510.1.

Danezis, C., Kakoullis, D., Fotiou, K., Chatzinikos, M., Kotsakis, C., Ioannou, G., et al., 2024. Enhancing geohazard resilience in Cyprus: the cyclops+ integrated GNSS and InSAR strategic monitoring infrastructure. In: IGARSS 2024, pp. 3802–3807.

Dehls, J.F., Larsen, Y., Marinkovic, P., Lauknes, T.R., Stødle, D., Moldestad, D.A., 2019. INSAR. No: a national InSAR deformation mapping/monitoring service in Norway–from concept to operations. In: IGARSS 2019, pp. 5461–5464.

Dehls, J.F., Kenyeres, A., Tóth, S., Larsen, Y., Marinkovic, P., 2022. Towards geodetically robust datum connection of large-scale InSAR results-EGMS perspective. In: IGARSS 2022, pp. 5097–5100.

Detektia, 2024. https://detektia.com/european-ground-motion-service (in Spanish).

Donnelly, L.J., 2000. Reactivation of geological faults during mining subsidence from 1859 to 2000 and beyond. Min. Technol. 109 (3), 179–190.

Donnelly, L.J., 2006. A review of coal mining induced fault reactivation in Great Britain. Q. J. Eng. Geol. Hydrogeol. 39 (1), 5–50.

Duchossois, G., Berdahl, M., Diehl, T., Garric, G., Humbert, A., Itkin, P., Jawak, S., Tietsche, S., 2024. Copernicus Polar Roadmap for Service Evolution. Publications Office of the European Union, Luxembourg, p. 68. https://doi.org/10.2889/644108.

EGMS White Paper, 2017. Available online: https://land.copernicus.eu/en/products/european-ground-motion-service/egms-white-paper.

Eskandari, R., Scaioni, M., 2023. European ground motion service for bridge monitoring: temporal and thermal deformation cross-check using Cosmo-Skymed InSAR. Int. Arch. Photogramm. Remote. Sens. Spat. Inf. Sci. 48, 1235–1241.

Eskandari, R., Scaioni, M., 2024. Spatiotemporal pattern detection of ground deformations induced by extreme rainfall using InSAR EGMS: the case of Cortina d'Ampezzo after Vaia storm. ISPRS Ann. Photogramm. Remote Sens. Spat. Inf. Sci. 10, 131–138.

Evelpidou, N., Ganas, A., Karkani, A., Spyrou, E., Saitis, G., 2023. Late quaternary relative sea-level changes and vertical GNSS motions in the Gulf of Corinth: the asymmetric localization of deformation inside an active half-graben. Geosciences 13 (11), 329.

Even, M., Westerhaus, M., Kutterer, H., Reubelt, T., Wolf, C., et al., 2024b. Ground motion services and monitoring of movements of the Earth's surface with InSAR–present developments and perspectives. ZfV-Zeitschrift für Geodäsie, Geoinformation und Landmanagement.
Evers, M., Thiele, A., Hammer, H., Hinz, S., 2023. PSDefoPAT—persistent Scatterer deformation pattern analysis tool. Remote Sens. 15 (19), 4646.
Evers, M., Vorwagner, A., Thiele, A., 2024. Deformation of the Schottwien bridge in Austria observed with the European ground motion service. In: IGARSS 2024, pp. 11119–11122.
Farías, C.A., Lenardón Sánchez, M., Bonì, R., Cigna, F., 2024. Statistical and independent component analysis of Sentinel-1 InSAR time series to assess land subsidence trends. Remote Sens. 16 (21), 4066.
Ferretti, A., Fumagalli, A., Novali, F., Prati, C., Rocca, F., Rucci, A., 2011. A new algorithm for processing interferometric data-stacks. SqueeSAR. IEEE TGRS 49 (9), 3460–3470.
Ferretti, A., Passera, E., Capes, R., 2025. Algorithm Theoretical Basis Document. EEA, p. 84. https://land.copernicus.eu/en/technical-library/egms-algorithm-theoretical-basis-document/@@download/file.
Festa, D., Del Soldato, M., 2023. EGMStream, a desktop app for EGMS data downstream. Remote Sens. 15 (10), 2581.
Ferretti, A., Prati, C., Rocca, F., 2000. Nonlinear subsidence rate estimation using permanent scatterers in differential SAR interferometry. IEEE Trans. Geosci. Remote Sens 38, 2202–2212. https://doi.org/10.1109/36.868878.
Ferretti, A., Prati, C., Rocca, F., 2001. Permanent scatterers in SAR interferometry. IEEE Trans. Geosci. Remote Sens. 39, 8–20. https://doi.org/10.1109/igarss.1999.772008.
Festa, D., Bonano, M., Casagli, N., Confuorto, P., De Luca, C., Del Soldato, M., et al., 2022. Nation-wide mapping and classification of ground deformation phenomena through the spatial clustering of P-SBAS InSAR measurements: Italy case study. ISPRS J. Photogramm. Remote Sens. 189, 1–22.
Fibbi, G., Beni, T., Fanti, R., Del Soldato, M., 2023. Underground gas storage monitoring using free and open source InSAR data: a case study from Yela (Spain). Energies 16 (17), 6392.
Fibbi, G., Beni, T., Del Soldato, M., Fanti, R., 2024. EGMS insights into ground deformation patterns in underground gas storage (UGS) activities. In: EGU General Assembly Conference Abstracts, EGU24-8610.
Ghaderpour, E., Mazzanti, P., Bozzano, F., Mugnozza, G.S., 2024. Ground deformation monitoring via PS-InSAR time series: an industrial zone in Sacco River Valley, central Italy. Remote Sens. Appl.: Soc. Environ. 4, 101191.
Ghaderpour, E., Scarascia Mugnozza, G., Mineo, S., Meisina, C., Pappalardo, G., 2024b. Ground deformation monitoring using InSAR and meteorological time series and least-squares wavelet software: a case study in Catania, Italy. Adv. Geosci. 64, 1–5.
Ghaderpour, E., Antonielli, B., Bozzano, F., Scarascia Mugnozza, G., Mazzanti, P., 2024c. Detecting trend turning points in PS-InSAR time series: slow-moving landslides in province of Frosinone, Italy. Eng. Proc. 68 (1), 12.
Godone, D., Allasia, P., Notti, D., Baldo, M., Poggi, F., Faccini, F., 2023. Coexistence of a marginal mountain community with large-scale and low kinematic landslide: the intensive monitoring approach. Remote Sens. 15 (13), 3238.
Guinau, M., Fernández-Jiménez, C., Barra, A., Vilaplana-Muzas, M., Flores, A., Ortuño, M., et al., 2024. Multi-technique analysis and landscape evolution: implications for landslide-fluvial cascading hazards assessment. In: EGU General Assembly Conference Abstracts, EGU24-14955.
Guzy, A., 2024. Subsidence and uplift in active and closed lignite mines: impacts of energy transition and climate change. Energies 17 (22), 5540.
Hasan, M.F., Smith, R., Vajedian, S., Pommerenke, R., Majumdar, S., 2023. Global land subsidence mapping reveals widespread loss of aquifer storage capacity. Nat. Commun. 14 (1), 6180.
Hlaváčová, I., Kolomazník, J., Struhár, J., Orlitová, E., 2023. InSAR ground motion mapping in support of urban resilience and regional landscape planning. In: 2023 Joint Urban Remote Sensing Event (JURSE), pp. 1–4.
Hooper, A., Zebker, H., Segall, P., Kampes, B., 2004. A new method for measuring deformation on volcanoes and other natural terrains using InSAR persistent scatterers. Geophys. Res. Lett. 31 (23).
Hourston, H., Álvarez, I.G., Bateson, L., Hussain, E., Novellino, A., 2024. Automated INSAR time-series analysis tool for geological interpretations in near-real time. In: IGARSS 2024, pp. 9971–9974.
Hrysiewicz, A., Khoshlahjeh Azar, M., Holohan, E.P., 2024. EGMS-toolkit: a set of Python scripts for improved access to datasets from the European ground motion service. Earth Sci. Inf. 1–13.
Ilieva, M., Pawłuszek-Filipiak, K., Teodorczyk, D., Wielgocka, N., Balak, P., Stasch, K., Tymków, P., et al., 2024. EPOS-PL+ project-infrastructure for long-term InSAR monitoring of mining induced deformations in Southern Poland. In: EGU General Assembly Conference Abstracts, EGU24-19176.
Intermap Technologies, 2007. NEXTMap British Digital Terrain Model Dataset Produced by Intermap. NERC Earth Observation Data Centre. http://catalogue.ceda.ac.uk/uuid/8f6e1598372c058f07b0aeac2442366d/.
Ioannidis, C., Verykokou, S., Soile, S., Istrati, D., Spyrakos, C., Sarris, A., Anyfantis, G.C., et al., 2024. Safeguarding our heritage—the TRIQUETRA project approach. Heritage 7 (2), 758–793.
IPCC, 2021. Sixth Assessment Report, Climate Change 2021: The Physical Science Basis. Available at https://www.ipcc.ch/assessment-report/ar6/.
Kalia, A.C., Frei, M., Lege, T., 2017. A Copernicus downstream-service for the nationwide monitoring of surface displacements in Germany. Remote Sens. Environ. 202, 234–249.
Khan, J., Rosi, A., Raj Meena, S., Floris, M., 2024. The role of artificial intelligence in modeling and predicting ground deformation using advanced InSAR data. In: EGU General Assembly Conference Abstracts, EGU24-13026.
Kotzerke, P., Siegmund, R., Langenwalter, J., 2022. Product User Manual. EEA, p. 56. https://land.copernicus.eu/en/technical-library/egms-product-user-manual/@@download/file.
Kotzerke, P., Siegmund, R., Larsen, Y., 2024. Quality Assurance & Control Report: Third Update. EEA, p. 13. https://land.copernicus.eu/en/technical-library/egms-quality-assurance-and-control-report/@@download/file.
Kuzu, R.S., Bagaglini, L., Wang, Y., Dumitru, C.O., Braham, N.A.A., Pasquali, G., et al., 2023. Automatic detection of building displacements through unsupervised learning from InSAR data. IEEE J. Sel. Top. Appl. Earth Obs. Remote Sens. 16, 6931–6947.
Lanari, R., Lundgren, P., Sansosti, E., 1998. Dynamic deformation of Etna volcano observed by satellite radar interferometry. Geophys. Res. Lett. 25, 1541–1544.
Larsen, Y., Marinkovic, P., Dehls, J.F., Bredal, M., Bishop, C., et al., 2020. European Ground Motion Service: Service Implementation Plan and Product Specification Document, p. 166. https://land.copernicus.eu/en/products/european-ground-motion-service/d2_d3_combined_sip_psd-1_01_final-1.pdf.
Larsen, Y., Marinkovic, P., Dehls, J., Stødle, D., 2023. End User Interface Manual, p. 24. https://land.copernicus.eu/en/technical-library/egms-end-user-interface-manual/@@download/file.
Lau, R., Seguí, C., Waterman, T., Chaney, N., Veveakis, M., 2024. InSAR-informed in situ monitoring for deep-seated landslides: insights from El Forn (Andorra). Nat. Hazards Earth Syst. Sci. 24 (10), 3651–3661.
Lauknes, T.R., Shanker, A.P., Dehls, J.F., Zebker, H.A., Henderson, I.H.C., Larsen, Y., 2010. Detailed rockslide mapping in northern Norway with small baseline and persistent scatterer interferometric SAR time series methods. Remote Sens. Environ. 114 (9), 2097–2109.
Lenardón Sánchez, M.L., Farías, C.A., Cigna, F., 2024. Multi-decadal land subsidence risk assessment at major Italian cities by integrating PSInSAR with urban vulnerability. Land 13 (12), 1–34.
Leone, G., Ginolfi, M., Esposito, L., Fiorillo, F., 2024. Terzaghi's effective stress principle and hydrological deformation of karst massifs detected by GNSS and InSAR. Ital. J. Eng. Geol. Environ. 185–195.
Lodigiani, D., Franzini, M., Casella, V., 2024. Improved analysis of EGMS data for displacement monitoring: the case study of Regina Montis Regalis basilica in Vicoforte, Italy. In: GISTAM, pp. 71–82.
Lundgren, P., Casu, F., Manzo, M., Pepe, A., Berardino, P., Sansosti, E., Lanari, R., 2004. Gravity and magma induced spreading of Mount Etna volcano revealed by satellite radar interferometry. Geophys. Res. Lett. 2004 (31), L04602.
Magnall, N., Ingleby, T., Douglas, S., 2024. Utilising InSAR for monitoring infrastructure at national scales. In: Proceedings of the 10th European Workshop on Structural Health Monitoring (EWSHM), e-Journal of Nondestructive Testing.
Malinowska, D., Milillo, P., Briggs, K., Reale, C., Giardina, G., 2024. Coherence-based prediction of multi-temporal InSAR measurement availability for infrastructure monitoring. IEEE J. Sel. Top. Appl. Earth Obs. Remote Sens. 17.
Marinkovic, P., Larsen, Y., Kenyeres, A., Tóth, S., 2024. GNSS Calibration Report, p. 31. https://land.copernicus.eu/en/technical-library/gnss-calibration-report/@@download/file.
Matano, F., Casaburi, A., De Natale, G., 2024. A Procedure for Analyzing Vertical Ground Deformation Anomalies in Active Volcanic Caldera during Unrest Phases. Preprints.org.
Mateos, R.M., Collados-Lara, A.J., Pulido-Velazquez, D., Baena-Ruiz, L., 2024. Assessing potential future subsidence due to groundwater depletion in "Alto Genil" basin (southern Spain). In: EGU General Assembly Conference Abstracts, EGU24-20678.
Medici, C., Novellino, A., Dashwood, C., Bianchini, S., 2024. Semi-automatic analysis of InSAR large datasets for landslide mapping and monitoring: the Great Britain case study. In: EGU General Assembly Conference Abstracts, EGU24-6191.
Medici, C., Becattini, F., Dashwood, C., Del Soldato, M., Bianchini, S., Bateson, L., Lee, K., Novellino, A., 2025. On the use of the EGMS data for studying landslides in Great Britain. In: Earth Observation Applications to Landslide Mapping, Monitoring and Modeling. Elsevier, pp. 71–86.
Mele, A., Crosetto, M., Miano, A., Prota, A., 2023. ADAFinder tool applied to EGMS data for the structural health monitoring of urban settlements. Remote Sens. 15 (2), 324.
Melet, A., et al., 2021. European Copernicus services to inform on sea-level rise adaptation: current status and perspectives. Front. Mar. Sci. 8, 703425.
Melichar, R., Baroň, I., Rowberry, M., Jelének, J., Sokol, Papí Isaba, M.D.P., Bürgmann, R., et al., 2024. Unusual fault kinematic behaviour and near-surface crustal stress variations before and during an earthquake series in the Vienna Basin (Austria) in spring 2021. In: EGU General Assembly Conference Abstracts, EGU24-7664.
Metzger, S., Aftab Uddin, M., Mouslopoulou, V., Begg, J., Nicol, A., Saltogianni, V., Oncken, O., 2023. Recent kinematics of crete, observed by InSAR, reveal complex, curved-forearc deformation and aquifers changes. In: EGU General Assembly Conference Abstracts, EGU-13785.
Mildon, Z., Diercks, M., Roberts, G., Walker, J.F., Ganas, A., Papanikolaou, I., Mitchell, S., et al., 2024. Transient aseismic vertical deformation during the interseismic cycle across the Pisia-Skinos normal fault (Gulf of Corinth, Greece). In: EGU General Assembly Conference Abstracts, EGU24-16153.
Milenova Vasileva, S., 2023. PS-DInSAR Processing of Sentinel-1 Images in the Hambach Mine, Germany, and its Applicability in Civil Infrastructure Monitoring. Master thesis. Universidad Pública de Navarra (Spain).
Motagh, M., Shamshiri, R., Haghighi, M.H., Wetzel, H.U., Akbari, B., Nahavandchi, H., Roessner, S., Arabi, S., 2017. Quantifying groundwater exploitation induced subsidence in the Rafsanjan plain, southeastern Iran, using InSAR time-series and in situ measurements. Eng. Geol. 218, 134–151.
Mora, O., Mallorqui, J.J., Broquetas, A., 2003. Linear and nonlinear terrain deformation maps from a reduced set of interferometric SAR images. IEEE TGRS 41 (10), 2243–2253.

Motagh, M., Haghighi, M.H., Piter, A., Vassileva, M., 2024. Mining-induced subsidence and fault reactivation due to open pit lignite mining in the Hambach region, North Rhine-Westphalia, Germany: insights from Sentinel-1 based European ground motion service (EGMS) and field surveys. In: EGU General Assembly Conference Abstracts, EGU24-11866.

Navarro, J.A., Tomás, R., Barra, A., Pagán, J.I., Reyes-Carmona, C., Solari, L., Vinielles, J. L., Falco, S., Crosetto, M., 2020. ADAtools: automatic detection and classification of active deformation areas from PSI displacement maps. Int. J. Geo-Inf. 9, 584.

Necula, N., Niculiță, M., 2023. Towards national active landslide inventory using EGMS datasets. Rev. Geomorfol. 25, 16.

Necula, N., Niculiță, M., 2024. Active landslides inventory update based on EGMS data for slowing moving landslides in a hilly environment. In: EGU General Assembly Conference Abstracts, EGU24-14387.

Negula, I.D., Moise, C., Dediu, F., Gheorghe, M., Tudor, G., Sefercik, U.G., 2023. Assessment of the European ground motion service ortho products for landfill systematic observation. Sci. Pap. Ser. E. Land Reclam. Earth Obs. Surv. Environ. Eng. 12.

Nikolakopoulos, K.G., Kyriou, A., Koukouvelas, I.K., Tomaras, N., Lyros, E., 2023. UAV, GNSS, and InSAR data analyses for landslide monitoring in a mountainous village in Western Greece. Remote Sens. 15 (11), 2870.

Nikolov, H., Atanasova, M., Atanasova-Zlatareva, M., 2023. Registering the ground deformations at the area of the archaeological site "Solnitsata". In: 5th Joint International Symposium on Deformation Monitoring, JISDM 2022, pp. 305–310.

ONS, 2020. Coastal towns in England and Wales: October 2020. https://www.ons.gov.uk/businessindustryandtrade/tourismindustry/articles/coastaltownsinenglandandwales/2020-10-06.

Palamà, R., Barra, A., Cuevas-González, M., Monserrat, O., Crosetto, M., 2024. Ground motion classification from European ground motion service data using extreme gradient boosting. In: IGARSS 2024, pp. 10736–10739.

Parenti, C., Grassi, F., Rossi, P., Soldati, M., Pattuzzi, E., Mancini, F., 2024. Synergistic use of synthetic aperture radar interferometry and geomorphological analysis in slow-moving landslide investigation in the northern Apennines (Italy). Land 13 (9), 1505.

Pawłuszek-Filipiak, K., Wielgocka, N., Tondaś, D., Borkowski, A., 2023. Monitoring nonlinear and fast deformation caused by underground mining exploitation using multi-temporal Sentinel-1 radar interferometry and corner reflectors: application, validation and processing obstacles. Int. J. Digit. Earth 16 (1), 251–271.

Petio, P., Massimi, V., Iasillo, D., Fazio, T., Forenza, G., Taggio, N., et al., 2024. Development of an operational infrastructure monitoring service for predictive maintenance based on Rheticus safeway. In: Earth Resources and Environmental Remote Sensing/GIS Applications XV, SPIE, 13197, pp. 214–222.

Pezzo, G., Palano, M., Beccaro, L., Tolomei, C., Albano, M., Atzori, S., Chiarabba, C., 2023. Coupling flank collapse and magma dynamics on stratovolcanoes: the Mt. Etna example from InSAR and GNSS observations. Remote Sens. 15, 847. https://doi.org/10.3390/rs15030847.

Pirotti, F., Toffah, F.E., Guarnieri, A., 2024. Correlation analysis of vertical ground movement and climate using Sentinel-1 InSAR. Remote Sens. 16 (22), 4123.

Piter, A., Haghshenas Haghighi, M., Motagh, M., 2024. Challenges and opportunities of Sentinel-1 InSAR for transport infrastructure monitoring. PFG–J. Photogramm. Remote Sens. Geoinf. Sci. 92, 609–627.

Rasà, R., Azzaro, R., Leonardi, O., 1996. Aseismic creep on faults and flank instability at Mount Etna volcano, Sicily. In: McGuire, W.C., Jones, A.P., Neuberg, J. (Eds.), Volcano Instability on the Earth and Other Planets, vol. 110. Geological Society, Special Publications, pp. 179–192. https://doi.org/10.1144/gsl.sp.1996.110.01.14.

Regione Piemonte, 2024. https://www.regione.piemonte.it/web/temi/protezione-civile-difesa-suolo-opere-pubbliche/geologia-prevenzione-rischio-geologico/frane-monitoraggio/monitoraggio-delle-frane-piemonte (in Italian).

Rigamonti, S., Dattola, G., Ciantia, M.O., Crosta, G.B., 2024. A multivariate time series analysis of underground gas storage deformations using InSAR data. In: EGU General Assembly Conference Abstracts, EGU24-19174.

Righini, M., Bonì, R., Sapio, S., Gatti, I., Salvadore, M., Taramelli, A., 2024. Development of a proof-of-concept A-DInSAR-based monitoring service for land subsidence. Remote Sens. 16 (11), 1981.

Rivera-Rivera, J.S., Béjar Pizarro, M., Aguilera Alonso, H., Ezquerro, P., Guardiola-Albert, C., Monserrat, O., 2024. Automated classification of ground deformation processes in Spain: a machine learning approach using a novel national InSAR-based database. In: EGU General Assembly Conference Abstracts, EGU24-8369.

Rodríguez-Antuñano, I., Martínez-Sánchez, J., Cabaleiro, M., Riveiro, B., 2023. Anticipating the collapse of urban infrastructure: a methodology based on earth observation and MT-InSAR. Remote Sens. 15 (15), 3867.

Rodríguez-Antuñano, I., Sousa, J.J., Bakoň, M., Ruiz-Armenteros, A.M., Martínez-Sánchez, J., Riveiro, B., 2024. Empowering intermediate cities: cost-effective heritage preservation through satellite remote sensing and deep learning. Int. J. Remote Sens. 45 (12), 4046–4074.

Rouyet, L., Lauknes, T.R., Christiansen, H.H., Strand, S.M., Larsen, Y., 2019. Seasonal dynamics of a permafrost landscape, Adventdalen, Svalbard, investigated by InSAR. Remote Sens. Environ. 231, 111236.

Rouyet, L., Bredal, M., Lauknes, T.R., Dehls, J., Larsen, Y., van Oostveen, J., Hindberg, H., Wendt, L., 2024. InSAR Svalbard – User Requirement, Technical Considerations, and Product Development Plan. Report no. 2-2024. NORCE Energy and Technology, p. 50. https://norceresearch.brage.unit.no/norceresearch-xmlui/handle/11250/3125660.

Ruch, J., Pepe, S., Casu, F., Solaro, G., Pepe, A., Acocella, V., et al., 2013. Seismo-tectonic behavior of the Pernicana fault system (Mt Etna): a gauge for volcano flank instability? J. Geophys. Res. Solid Earth 118, 4398–4409. https://doi.org/10.1002/jgrb.50281.

Rudolf, M., Krzepek, K., Homuth, B., Henk, A., Iwaszczuk, D., 2024. Identification and analysis of anomalous ground movements in urban and rural areas using persistent Scatterer Interferometry in southern Hesse, Germany. IEEE J. Sel. Top. Appl. Earth Obs. Remote Sens. 17, 10967–10978.

Ruiz-Armenteros, A.M., Marchamalo-Sacristán, M., Lamas-Fernández, F., Hernández-Cabezudo, Á., Delgado-Blasco, J.M., Bakon, M., Sousa, J.J., et al., 2023. Utilizing the land monitoring Copernicus program as a regular method for observing dams, large ponds, and surrounding areas. In: IGARSS 2023, pp. 8010–8013.

Ruiz-Armenteros, A.M., Marchamalo-Sacristán, M., Lamas-Fernández, F., Delgado-Blasco, J.M., Jurado-Rodríguez, J.M., Jurado-Rodríguez, D., et al., 2024. Routine monitoring of hydraulic infrastructures using the European ground motion service and other satellite radar sensors. Procedia Comput. Sci. 239, 2308–2315.

Sala, J., Vradi, A., Vöge, M., Raucoules, D., de Michele, M., Martins, J., Andersen, H.S., et al., 2023. European ground motion service validation: InSAR big data analytics. In: IGARSS 2023, pp. 2394–2397.

Sánchez-Fernández, J., Fernández-Landa, A., Hernández Cabezudo, Á., Molina Sánchez, R., 2024. Interferometric synthetic aperture radar phase linking with level 2 coregistered single look complexes: enhancing infrastructure monitoring accuracy at Algeciras port. Remote Sens. 16 (21), 3966.

Shahbazi, S., Crosetto, M., Barra, A., 2022. Ground deformation analysis using basic products of the Copernicus ground motion service. Int. Arch. Photogramm. Remote. Sens. Spat. Inf. Sci. 43, 349–354.

Shahbazi, S., Barra, A., Gao, Q., Crosetto, M., 2024. Detection of buildings with potential damage using differential deformation maps. ISPRS J. Photogramm. Remote Sens. 218, 57–69.

Shahbazi, S., Barra, A., Navarro, J.A., Crosetto, M., 2025. From EGMS to potential damage maps: assessing the potential impact of ground motion on exposed buildings. IEEE J. Sel. Top. Appl. Earth Obs. Remote Sens. 18, 26699–26715.

Siegmund, R., Kotzerke, P., Langenwalter, J., Berns, A., 2024. Utilisation of EGMS data in Alpine terrain-focussing on infrastructure under changing climate conditions. In: IGARSS 2024, pp. 4010–4013.

Simeone, V., Doglioni, A., D'Ambrosio, G., Fiorentino, A., Nitti, D.O., Nutricato, R., Guerricchio, A., 2024. Nutcracker deformation of arch bridge in consequence of slow gravitational slope deformations. Procedia Struct. Integrity 62, 561–568.

Solari, L., Del Soldato, M., Montalti, R., Bianchini, S., Raspini, F., Thuegaz, P., et al., 2019. A Sentinel-1 based hot-spot analysis: landslide mapping in North-Western Italy. Int. J. Remote Sens. 40 (20), 7898–7921.

Solarte, A., Reale, D., Sansosti, E., Fornaro, G., 2024. Advanced DInSAR data analysis for slow-moving landslide characterization. In: IGARSS 2024, pp. 11062–11065.

Sonnessa, A., 2024. Using SAR observation data to support the spatial planning in areas affected by landslide phenomena. In: Marucci, A., Zullo, F., Fiorini, L., Saganeiti, L. (Eds.), Innovation in Urban and Regional Planning. INPUT 2023. Lecture Notes in Civil Engineering, vol. 467. Springer, Cham.

Strade & Autostrade, 2024. https://www.stradeeautostrade.it/tecnologie-e-sistemi/il-dato-satellitare-storia-e-sviluppo/ (in Italian).

Strøm, G.D., Moldestad, D.A., Øydvin, E.K., Dehls, J., Bjordal, H., Fevang, P.A., 2014. Kartlegging og overvåkning av skredfare og infrastruktur ved bruk av radarsatellitter og InSAR metodikk. Grunnlag for en strategisk plan for offentlig bruk av interferometri i Norge. NRS rapport (2014)2. Norwegian Space Agency (In Norwegian).

Tang, W., Motagh, M., Zhan, W., 2020. Monitoring active open-pit mine stability in the Rhenish coalfields of Germany using a coherence-based SBAS method. Int. J. Appl. Earth Obs. Geoinf. 93, 102217.

Tarquini, S., Isola, I., Favalli, M., Battistini, A., Dotta, G., 2023. TINITALY, a Digital Elevation Model of Italy with a 10 Meters Cell Size (Version 1.1). Istituto Nazionale di Geofisica e Vulcanologia (INGV). https://doi.org/10.13127/tinitaly/1.1.

Thiéblemont, R., Le Cozannet, G., Nicholls, R.J., Rohmer, J., Wöppelmann, G., Raucoules, D., de Michele, M., Toimil, A., Lincke, D., 2024. Assessing current coastal subsidence at continental scale: insights from Europe using the European ground motion service. Earth's Future 12 (8).

Tibaldi, A., Groppelli, G., 2002. Volcano-tectonic activity along structures of the unstable NE flank of Mt. Etna (Italy) and their possible origin. J. Volcanol. Geotherm. Res. 115 (3–4), 277–302. https://doi.org/10.1016/S0377-0273(01)00305-5.

Tinagli, L., La Rosa, A., Paoli, G., 2024. Spatial and temporal evolution of mining-induced sinkholes in the Gavorrano area (Tuscany, Italy): insights from remote sensing and field data. Geomorphology 453, 109137.

Tondi, E., Patruno, J., Blasco, J.D., Catracchia, S., 2024. Analysis of the risk of subsidence of peripheral archaeological areas. In: IGARSS 2024, pp. 3366–3370.

Tonelli, D., Caspani, V.F., Valentini, A., Rocca, A., Torboli, R., Vitti, A., Zonta, D., et al., 2023. Interpretation of bridge health monitoring data from satellite InSAR technology. Remote Sens. 15 (21), 5242.

Torre, D., Galve, J.P., Reyes-Carmona, C., Alfonso-Jorde, D., Ballesteros, D., Menichetti, M., , et al.Azañón, J.M., 2024. Geomorphological assessment as basic complement of InSAR analysis for landslide processes understanding. Landslides 1–20.

Tzampoglou, P., Loupasakis, C., 2023. Hydrogeological hazards in open pit coal mines–investigating triggering mechanisms by validating the European ground motion service product with ground truth data. Water 15 (8), 1474.

Vassileva, M., Al-Halbouni, D., Motagh, M., Walter, T.R., Dahm, T., Wetzel, H.U., 2021. A decade-long silent ground subsidence hazard culminating in a metropolitan disaster in Maceió, Brazil. Sci. Rep. 11 (1), 7704.

Wang, Z., 2023. Risk Evaluation of Ground Motion using Machine Learning Models for the Lombardy Infrastructure. Master Thesis. Politecnico di Milano (Italy).

Werner, C., Wegmüller, U., Strozzi, T., Wiesmann, A., 2003. Interferometric point target analysis for deformation mapping. Proceedings of IGARSS 2003, Toulouse, France.

Yang, C.H., Stemmler, C., Müterthies, A., 2023. Ground movement analysis in post-Mining city using MTInSAR with help of European ground motion service. ISPRS Ann. Photogramm. Remote Sens. Spat. Inf. Sci. 10, 739–745.
Yishu, Y., 2022. Assessment of Landslides in Sondrio Province, Italy Based on EGMS: European Ground Motion Service. Master Thesis. Politecnico di Milano (Italy).
Zêzere, J.L., Mileu, N., Oliveira, S., Garcia, R., Melo, R., Santos, P., Reis, E., 2024. ADA Impact Tools User Manual. Deliverable D5.2 of the RASTOOL Project. https://rastool.cttc.es.
Zuccarini, A., Giacomelli, S., Severi, P., Berti, M., 2024. Long-term spatiotemporal evolution of land subsidence in the urban area of Bologna, Italy. Bull. Eng. Geol. Environ. 83 (1), 35.